# Electronic Supplementary Information

The structurally variable network of spin couplings and migrating paramagnetic centers in the binuclear *o*-quinone Co^{II} complexes with the biradical acene linkers: a computational DFT study

Vladimir I. Minkin, Andrey G. Starikov, Alyona A. Starikova, Ruslan M. Minyaev and Alexander. I. Boldyrev

_o_-Quinone derivatives of the acenes Q1 and complexes I

Table S1. Multiplicities (_Ms_), total energies (_E_), relative energies (ΔE), expectation values of the spin-squared operator (S^2) and spin coupling constants (J ([C]$_n$-[C]$_n$)) in the compounds **Q1** (n=1–7) calculated by DFT UB3LYP/6-311++G(d,p) method.

| Structure	_Ms_	E_{total}, a. u.	ΔE, kcal mol^{-1}	S^2	J ([C]$_n$-[C]$_n$), cm^{-1}
Q1 (n=1)	1	-1457.67922	–	0.000	–
Q1 (n=3)	1	-1765.01682	–	0.000	–
Q1 (n=5)	3	-2072.34181		2.036	-1869
BS	1	-2072.35272	6.8	0.755	
Q1 (n=6)	3	-2226.01500		2.039	-1885
BS	1	-2226.02352	5.3	1.046	
Q1 (n=7)	3	-2379.68640		2.041	-2087
BS	1	-2379.69401	4.8	1.241	
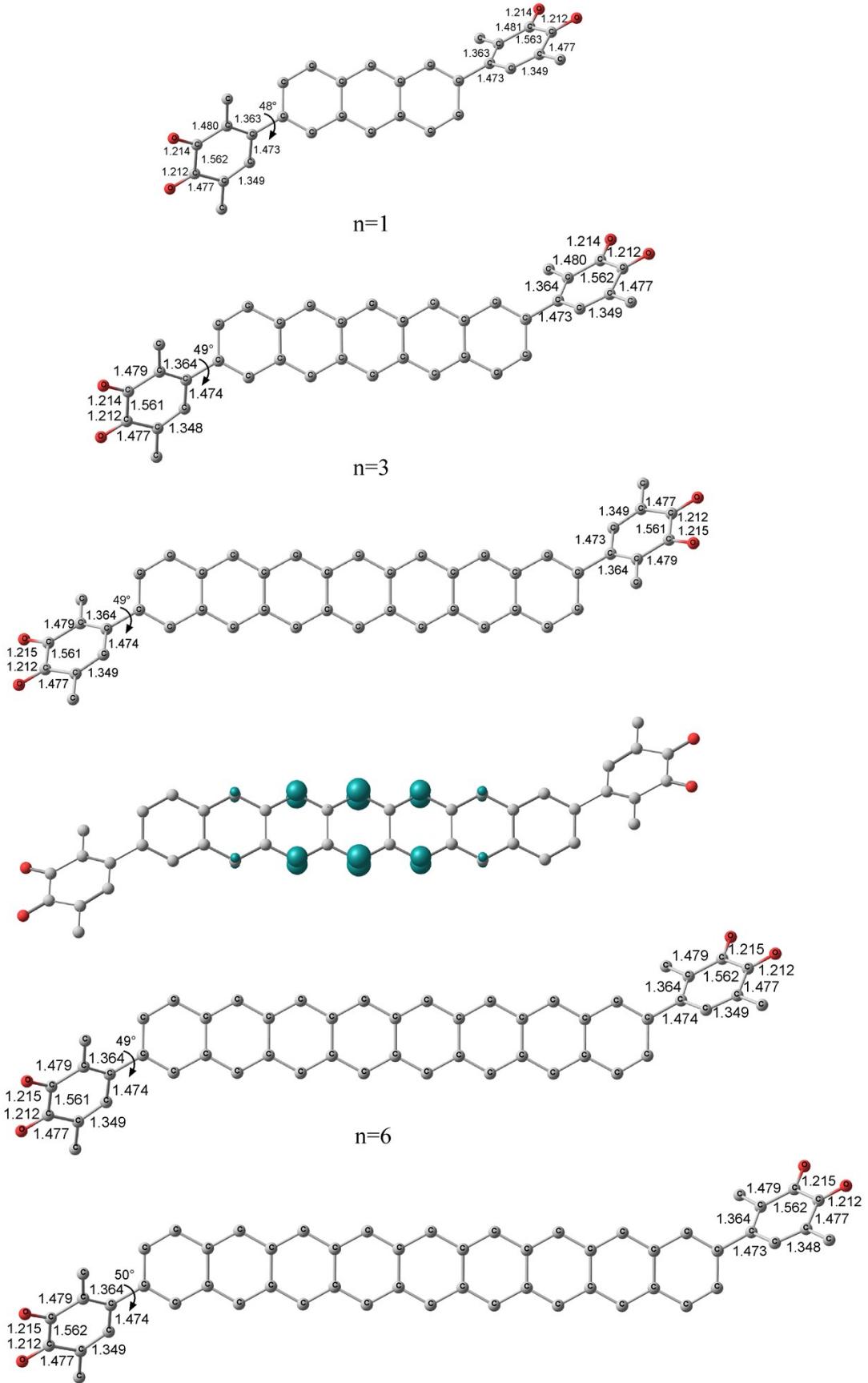
Figure S1. Optimized geometries of the compounds **Q1** (n=1–7) and spin density distribution in the **Q1** (n=5) calculated by DFT UB3LYP/6-311++G(d,p) method. Hereinafter hydrogen atoms are omitted for clarity, bond lengths are given in Å, spin density plots correspond to the spin states with maximum multiplicity.

Table S2. Multiplicities (*Ms*), total energies without (E_{total}) and with taking into account for energies of zero-point harmonic vibrations (E_{total}^{ZPE}), expectation values of the spin-squared operator (S^2) in the electromers of the adducts **I** (R_1, R_2 = CH_3, CF_3; n = 1) calculated by DFT UB3LYP*/6-311++G(d,p) method.

Structure	*Ms*	E_{total}, a. u.	E_{total}^{ZPE}, a. u.	S^2
$R_1 = R_2 = CH_3$				
1	3	-5580.17914	-5579.31792	2.012
1 BS	1	-5580.17925		1.009
2	5	-5580.15798	-5579.30049	6.393
2 BS	3	-5580.15791		3.392
3	7	-5580.13631	-5579.28275	12.820
3 BS	1	-5580.13636		3.822
$R_1 = CH_3, R_2 = CF_3$				
4	3	-6765.61871	-6764.84720	2.011
4 BS	1	-6765.61884		1.009
5	5	-6765.60598	-6764.83803	6.156
5 BS	3	-6765.60592		3.154
6	7	-6765.59209	-6764.82802	12.342
6 BS	1	-6765.59210		3.344
$R_1 = R_2 = CF_3$				
7	3	-7951.03874	-7950.35655	2.012
7 BS	1	-7951.03892		1.007
8	5	-7951.03465	-7950.35586	6.071
8 BS	3	-7951.03460		3.068
9	7	-7951.02898	-7950.35376	12.147
9 BS	1	-7951.02898		3.148
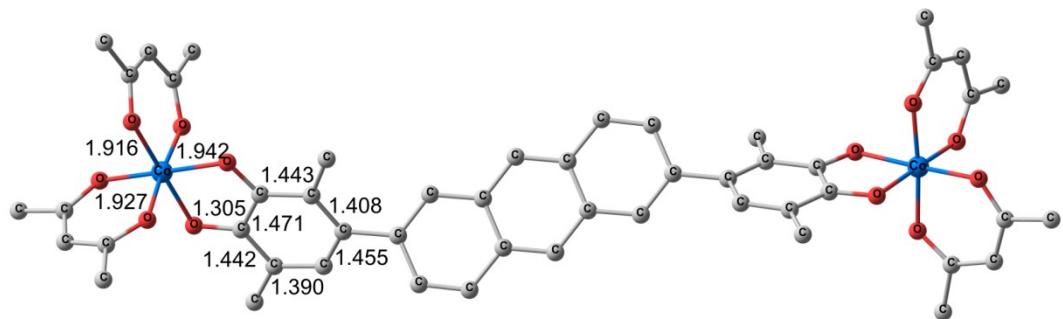
1 $_{LS}Co^{III}SQ$-$[C]_n$-$[C]_n$-$SQ_{LS}Co^{III}$
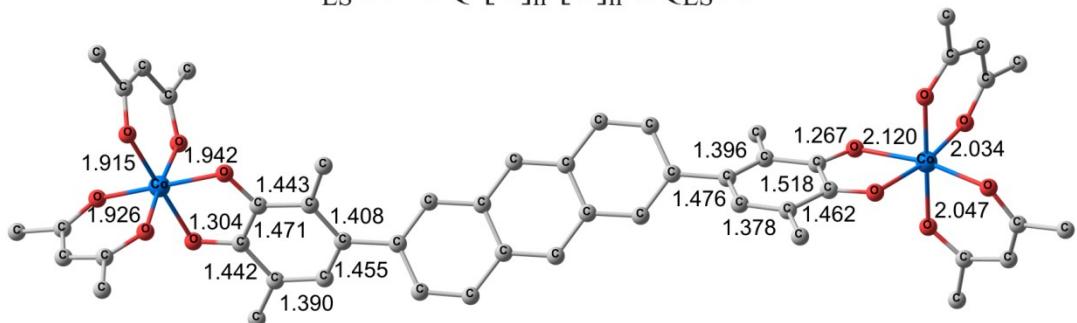
2 $_{LS}Co^{III}SQ$-$[C]_n$-$[C]_n$-$Q_{HS}Co^{II}$
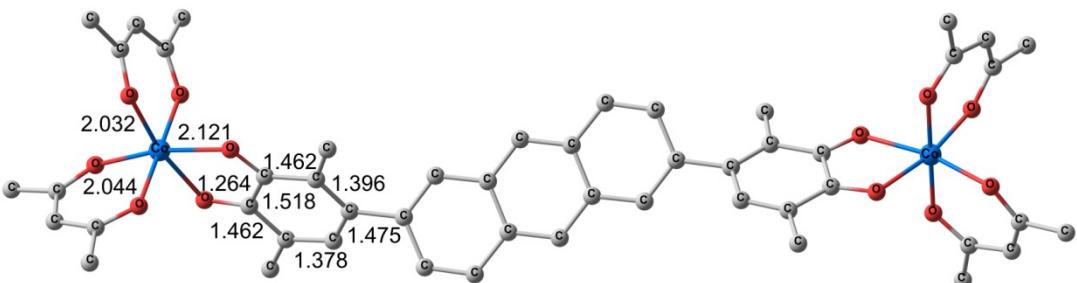

3 $_{HS}Co^{II}Q$-$[C]_n$-$[C]_n$-$Q_{HS}Co^{II}$

Figure S2. Optimized geometries of the electromers of the adduct **I** (R_1 = R_2 = CH_3; n = 1) calculated by DFT UB3LYP*/6-311++G(d,p) method.
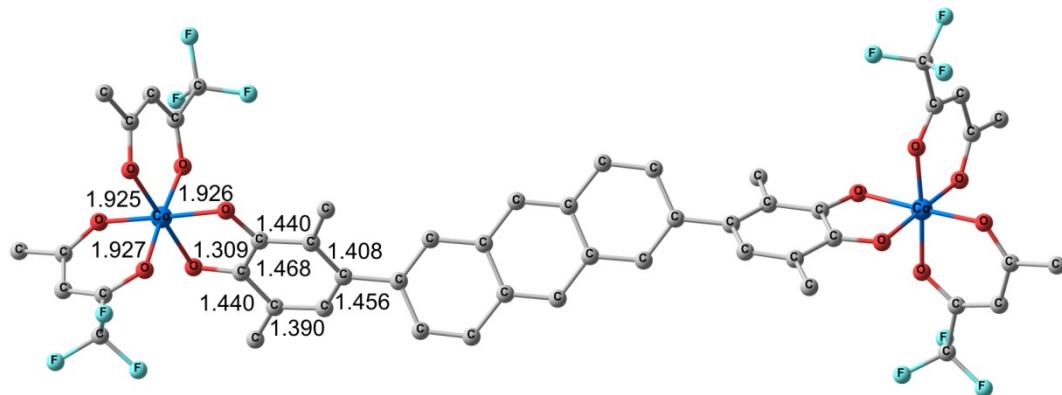
**4** LSCo^IIISQ-[C]_n-[C]_n-SQLSCo^III
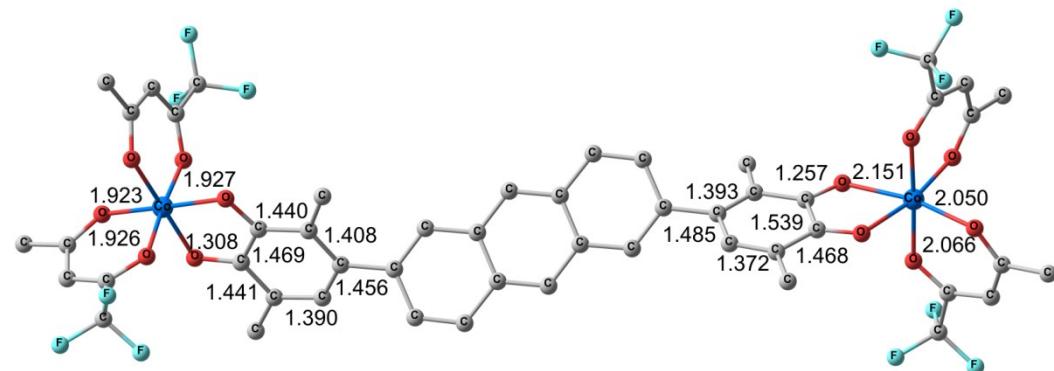
**5** LSCo^IIISQ-[C]_n-[C]_n-Q_HSCo^II
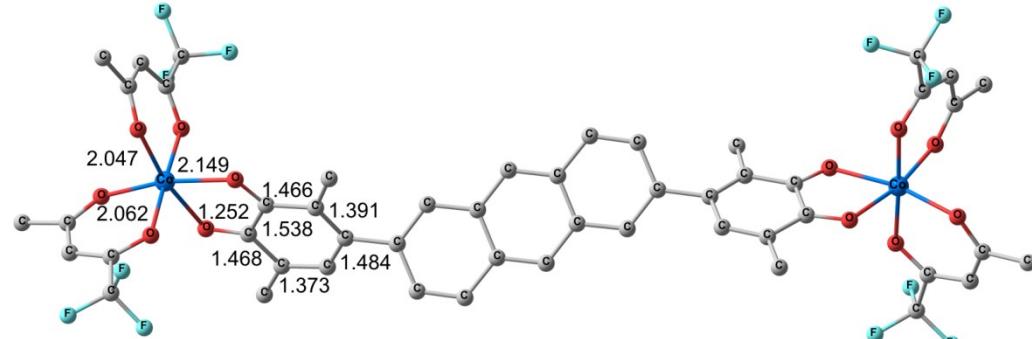
6 HSCo^IIQ-[C]_n-[C]_n-Q_HSCo^II

Figure S3. Optimized geometries of the electromers of the adduct **I** ($R_1 = CH_3$, $R_2 = CF_3$; $n = 1$) calculated by DFT UB3LYP*/6-311++G(d,p) method.
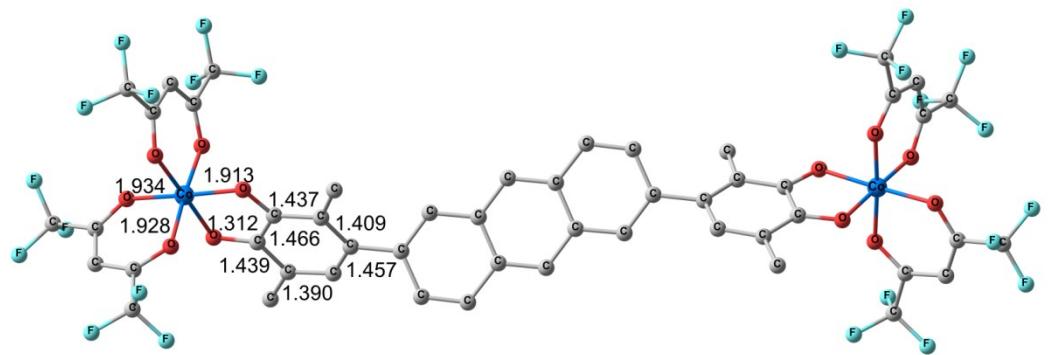
7 LSCoIIISQ-[C]n-[C]n-SQLSCoIII
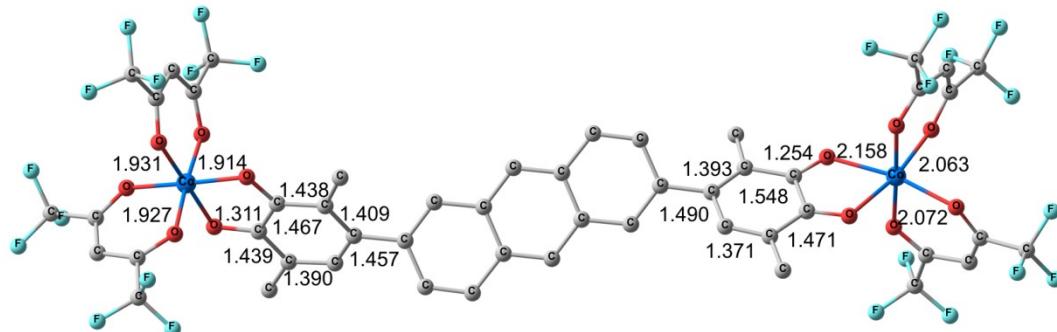
8 LSCoIIISQ-[C]n-[C]n-QHSCoII
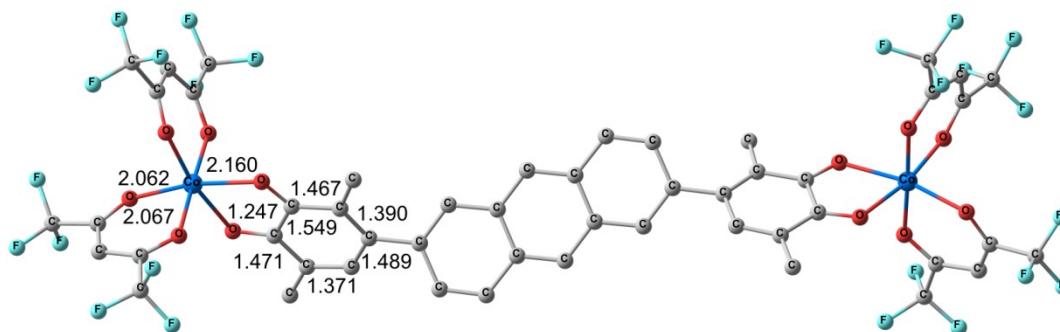
9 HSCoIIQ-[C]n-[C]n-QHSCoII

Figure S4. Optimized geometries of the electromers of the adduct **I** ($R_1 = R_2 = CF_3$; n = 1) calculated by DFT UB3LYP*/6-311++G(d,p) method.

Table S3. Multiplicities (Ms), total, stabilization and relative energies without (E_{total}, E_{stab}, ΔE) and with (E_{total}^{ZPE}, E_{stab}^{ZPE}, ΔE^{ZPE}) taking into account for energies of zero-point harmonic vibrations, exchange spin coupling constants (J), expectation values of the spin-squared operator (S^2) in the electromers of the adducts **I** (R_1, R_2 = CH_3, CF_3; n = 3) calculated by DFT UB3LYP*/6-311++G(d,p) method.

Structure	Ms	E_{total} (E_{total}^{ZPE}), a. u.	E_{stab} (E_{stab}^{ZPE}), kcal mol^{-1}	ΔE (ΔE^{ZPE}), kcal mol^{-1}	J, cm^{-1}	S^2
		R_1 = R_2 = CH_3				
10	3	-5885.37503 (-5884.42462)	36.9 (31.8)	0.0 (0.0)	−20	2.013
10 BS	1	-5885.37516				1.023
11	5	-5885.35426 (-5884.40763)	23.8 (21.1)	13.0 (10.7)	6	6.382
11 BS	3	-5885.35419				3.372
12	7	-5885.33256 (-5884.38972)	10.2 (9.9)	26.7 (21.9)	0	12.789
12 BS	1	-5885.33256				3.322
		R_1 = CH_3, R_2 = CF_3				
13	3	-7070.81467 (-7069.95407)	37.6 (32.2)	0.0 (0.0)	−28	2.012
13 BS	1	-7070.81484				1.007
14	5	-7070.80288 (-7069.94595)	30.2 (27.1)	7.4 (5.1)	5	6.150
14 BS	3	-7070.80281				3.154
15	7	-7070.78940 (-7069.93597)	21.7 (20.9)	15.9 (11.4)	0	12.311
15 BS	1	-7070.78940				3.336
		R_1 = R_2 = CF_3				
16	3	-8256.23534 (-8255.46405)	39.9 (34.4)	0.0 (0.0)	−35	2.012
16 BS	1	-8256.23550				1.007
17	5	-8256.23267 (8255.46491)	38.2 (34.9)	1.5 (−0.5)	7	6.083
17 BS	3	-8256.23259				3.068
18	7	-8256.22786 (-8255.46329)	35.2 (33.9)	4.7 (0.5)	0	12.132
18 BS	1	-8256.22786				3.148
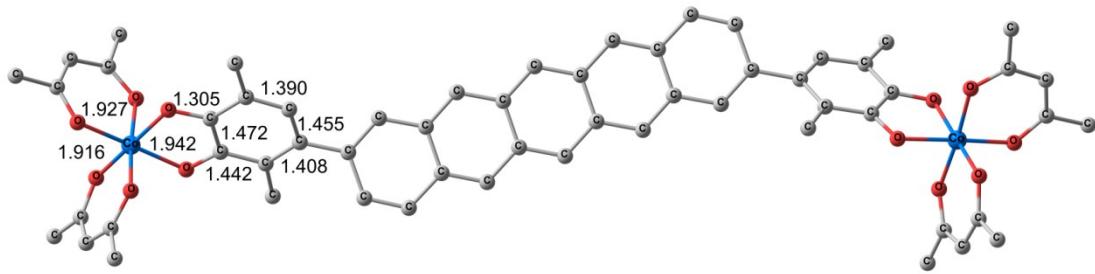
10 $_{LS}Co^{III}SQ$-[C]$_n$-[C]$_n$-SQ$_{LS}Co^{III}$
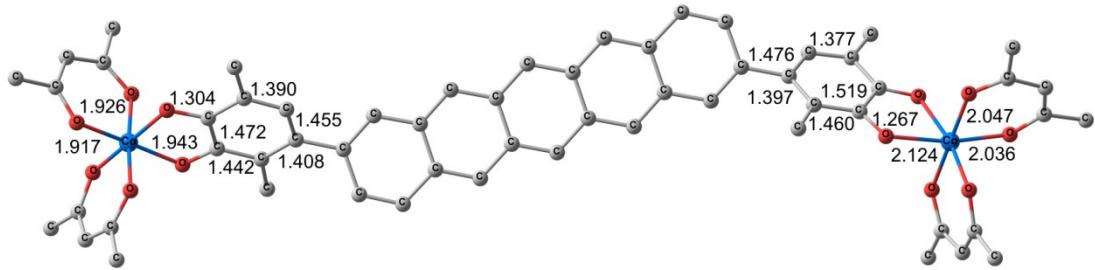
11 $_{LS}Co^{III}SQ$-[C]$_n$-[C]$_n$-Q$_{HS}Co^{II}$
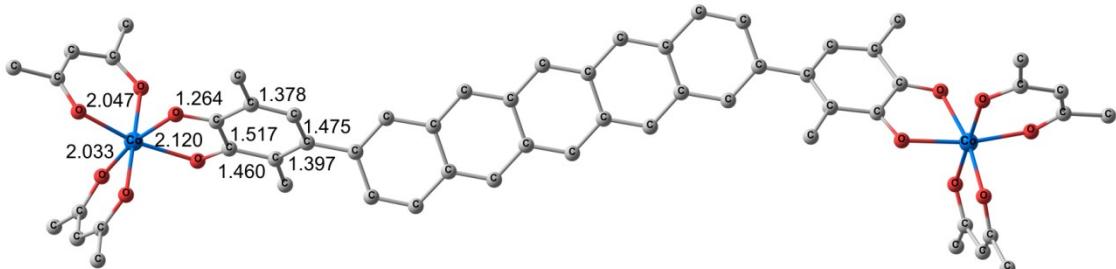

12 $_{HS}Co^{II}Q$-[C]$_n$-[C]$_n$-Q$_{HS}Co^{II}$

Figure S5. Optimized geometries of the electromers of the adduct **I** (R$_1$ = R$_2$= CH$_3$; n = 3) calculated by DFT UB3LYP*/6-311++G(d,p) method.
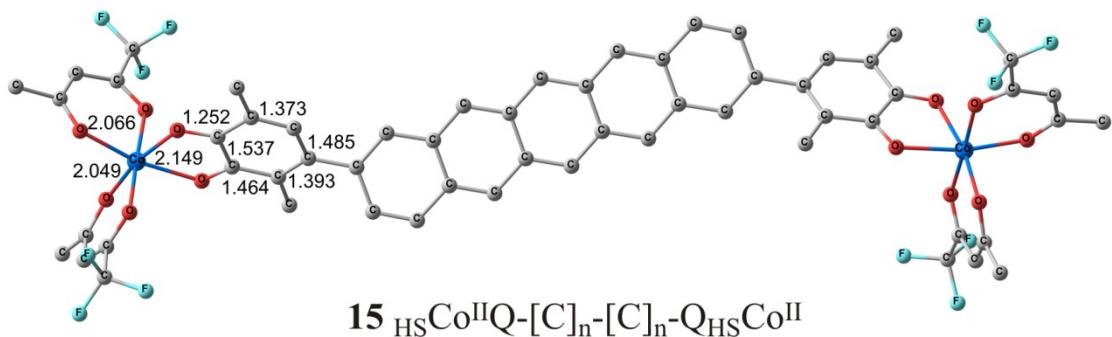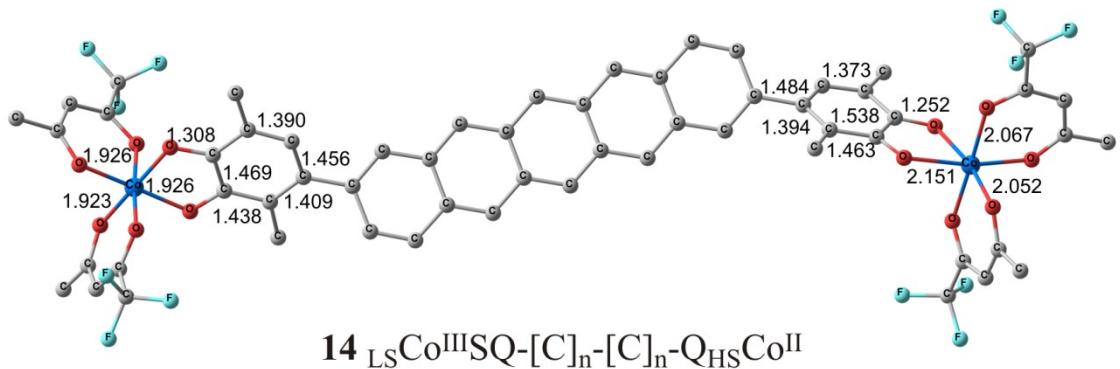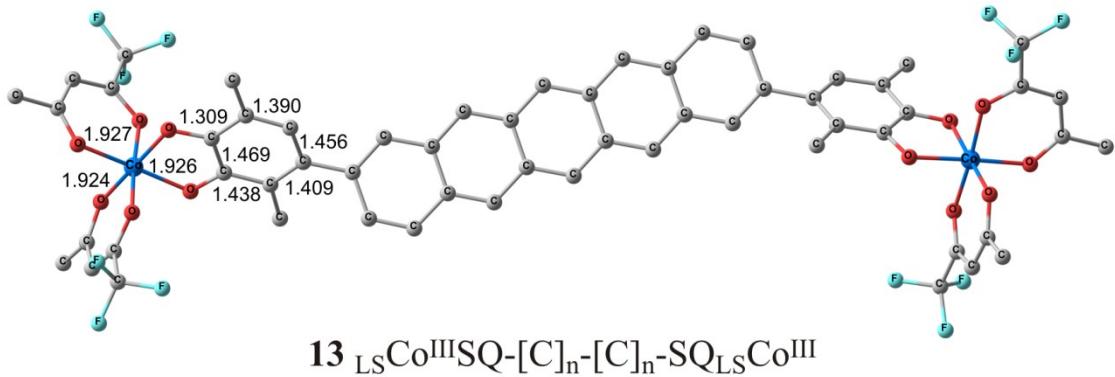
Figure S6. Optimized geometries of the electromers of the adduct **I** ($R_1 = CH_3$, $R_2 = CF_3$; $n = 3$) calculated by DFT UB3LYP*/6-311++G(d,p) method.
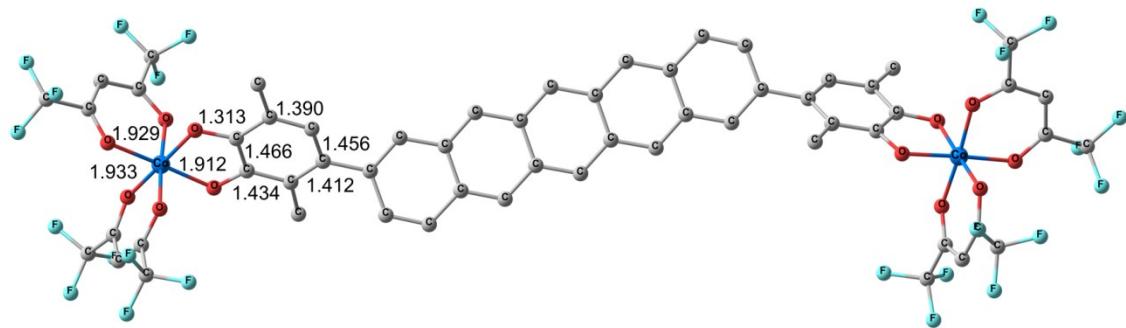
16 $_{LS}Co^{III}SQ$-$[C]_n$-$[C]_n$-$SQ_{LS}Co^{III}$
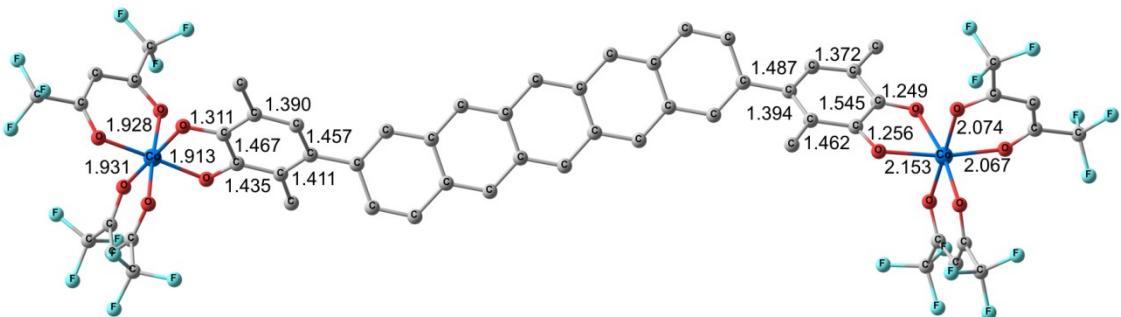
17 $_{LS}Co^{III}SQ$-$[C]_n$-$[C]_n$-$Q_{HS}Co^{II}$
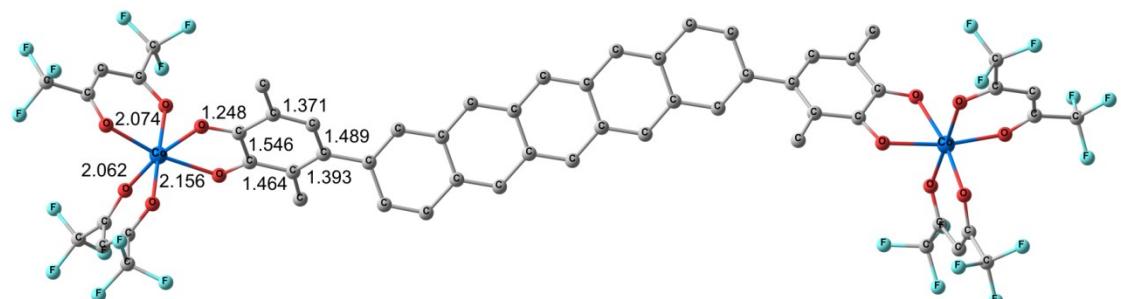
18 $_{HS}Co^{II}Q$-$[C]_n$-$[C]_n$-$Q_{HS}Co^{II}$

Figure S7. Optimized geometries of the electromers of the adduct **I** (R_1 = R_2 = CF_3; n = 3) calculated by DFT UB3LYP*/6-311++G(d,p) method.

Table S4. Multiplicities (Ms), total energies without (E_{total}) and with taking into account for energies of zero-point harmonic vibrations (E_{total}^{ZPE}), expectation values of the spin-squared operator (S^2) in the electromers of the adducts **I** (R_1, R_2 = CH_3, CF_3; n = 5) calculated by DFT UB3LYP*/6-311++G(d,p) method.

| Structure	Ms	E_{total}, a. u.	E_{total}^{ZPE}, a. u.	S^2
R_1 =R_2 = CH_3				
19 αααα*	5	-6190.55708	-6189.51930	6.037
αβαα=ααβα	3	-6190.56852		2.415
βααα=αααβ	3	-6190.55807		2.952
ααββ=αβαβ	1	-6190.56945		1.484
αββα	1	-6190.55912		1.879
20 αααα	7	-6190.53761	-6189.50335	12.325
αβαα=ααβα	5	-6190.54833		6.846
βααα	5	-6190.53823		7.271
ββαα=βαβα	3	-6190.54750		3.749
αββα	1	-6190.53746		4.294
αααβ	1	-6190.53660		3.354
21 αααα	9	-6190.51681	-6189.48637	20.715
αβαα=ααβα	7	-6190.52583		12.769
αββα	5	-6190.51540		8.746
βααα	3	-6190.51600		5.732
αβαβ=βαβα	1	-6190.52669		4.266
R_1 = CH_3, R_2 = CF_3				
22 αααα	5	-7375.99656	-7375.04867	6.037
αβαα=ααβα	3	-7376.00838		2.375
βααα=αααβ	3	-7375.99837		2.872
ααββ=αβαβ	1	-7376.00962		1.462
αββα	1	-7375.99980		1.770
23 αααα	7	-7375.98734	-7375.04273	12.219
αβαα=ααβα	5	-7375.99760		6.598
βααα	5	-7375.98858		7.043
ββαα=βαβα	3	-7375.99663		3.465
αββα	1	-7375.98782		4.047
αααβ	1	-7375.98656		3.128
24 αααα	9	-7375.97499	-7375.03410	20.131
αβαα=ααβα	7	-7375.98403		12.670
αββα	5	-7375.97390		8.281
βααα	3	-7375.97447		5.276
αβαβ=βαβα	1	-7375.98445		3.763

R₁ = R₂ = CF₃				
25 $\alpha\alpha\alpha\alpha$	5	-8561.41688	-8560.55838	6.037
$\alpha\beta\alpha\alpha=\alpha\alpha\beta\alpha$	3	-8561.42961		2.280
$\beta\alpha\alpha\alpha=\alpha\alpha\alpha\beta$	3	-8561.42004		2.761
$\alpha\alpha\beta\beta=\alpha\beta\alpha\beta$	1	-8561.43126		1.411
$\alpha\beta\beta\alpha$	1	-8561.42230		1.595
26 $\alpha\alpha\alpha\alpha$	7	-8561.41887	-8560.56335	12.072
$\alpha\beta\alpha\alpha=\alpha\alpha\beta\alpha$	5	-8561.42854		6.530
$\beta\alpha\alpha\alpha$	5	-8561.42023		6.945
$\beta\beta\alpha\alpha=\beta\alpha\beta\alpha$	3	-8561.42804		3.455
$\alpha\beta\beta\alpha$	1	-8561.41947		3.938
$\alpha\alpha\alpha\beta$	1	-8561.41800		3.072
27 $\alpha\alpha\alpha\alpha$	9	-8561.41578	-8560.56376	20.131
$\alpha\beta\alpha\alpha=\alpha\alpha\beta\alpha$	7	-8561.42371		12.516
$\alpha\beta\beta\alpha$	5	-8561.41487		8.131
$\beta\alpha\alpha\alpha$	3	-8561.41519		5.136
$\alpha\beta\alpha\beta=\beta\alpha\beta\alpha$	1	-8561.42408		3.600

[*]α corresponds to spin-up, β corresponds to spin-down; the ordering of the paramagnetic centers:
(1) SQ (2) $[C]_n$ (3) $[C]_n$ (4) SQ in the electromers $_{LS}Co^{III}SQ$-$[C]_n$-$[C]_n$-$SQ_{LS}Co^{III}$;

(1) SQ (2) $[C]_n$ (3) $[C]_n$ (4) $_{HS}Co^{II}$ in the electromers $_{LS}Co^{III}SQ$-$[C]_n$-$[C]_n$-$Q_{HS}Co^{II}$;

(1) $_{HS}Co^{II}$ (2) $[C]_n$ (3) $[C]_n$ (4) $_{HS}Co^{II}$ in the electromers $_{HS}Co^{II}Q$-$[C]_n$-$[C]_n$-$Q_{HS}Co^{II}$
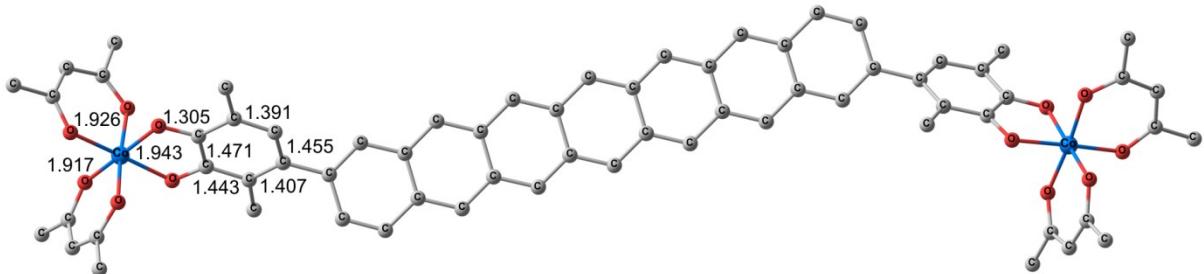
19 LSCoIIISQ-[C]n-[C]n-SQLSCoIII
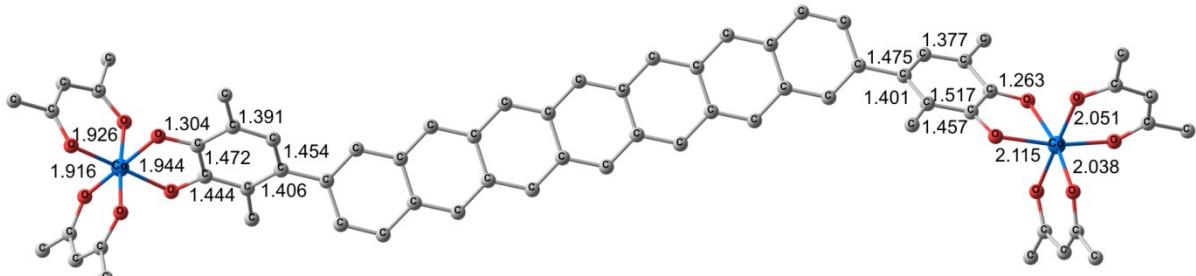
20 LSCoIIISQ-[C]n-[C]n-QHSCoII
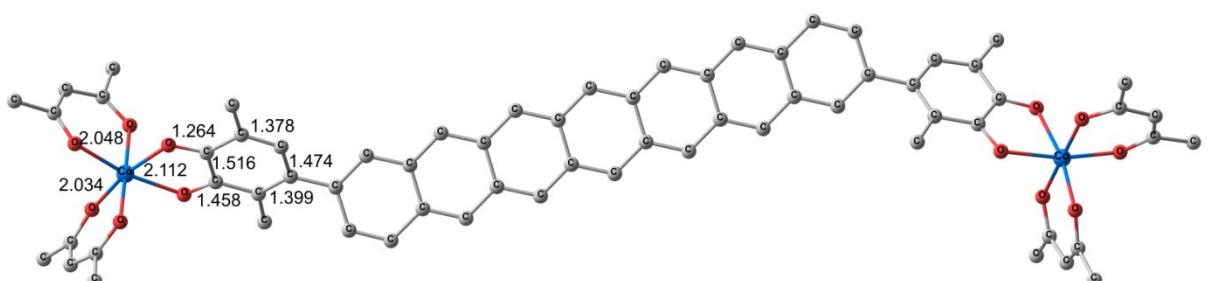
21 HSCoIIQ-[C]n-[C]n-QHSCoII

Figure S8. Optimized geometries of the electromers of the adduct **I** ($R_1 = R_2 = CH_3$; n = 5) calculated by DFT UB3LYP*/6-311++G(d,p) method.
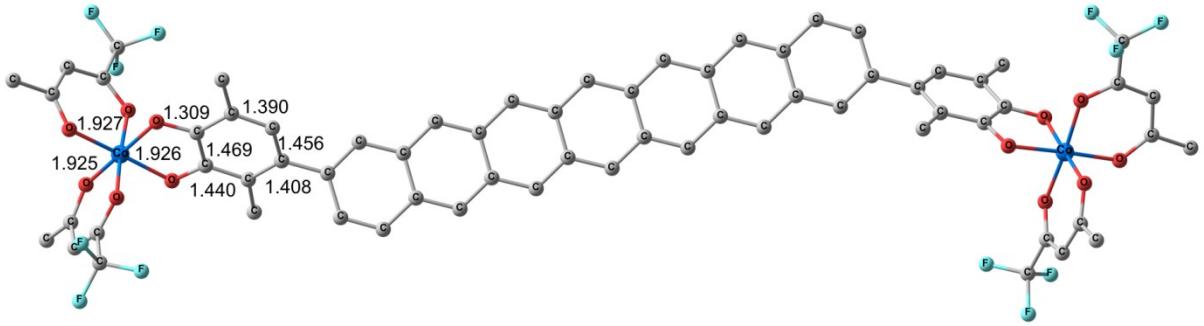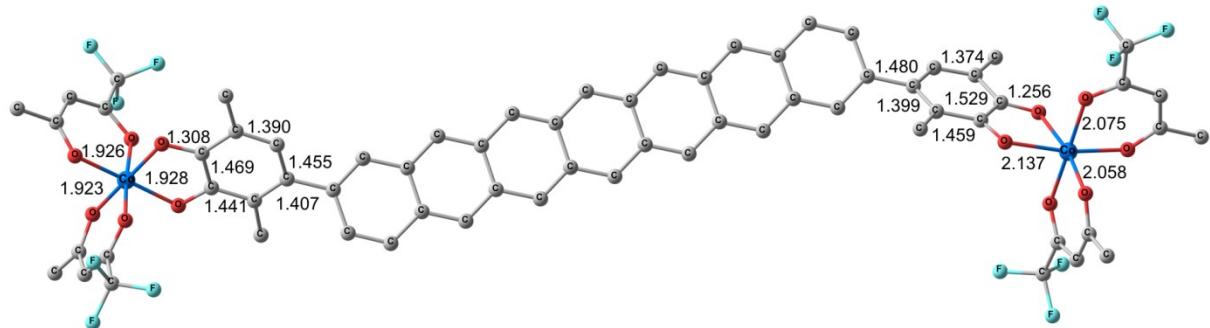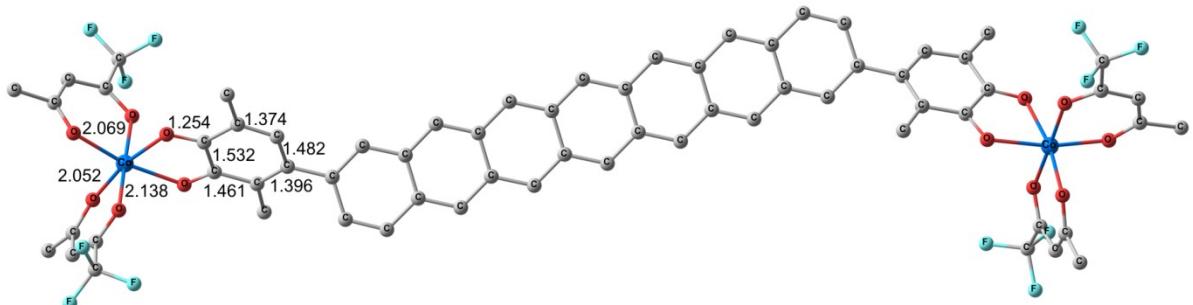
Figure S9. Optimized geometries of the electromers of the adduct **I** ($R_1 = CH_3$, $R_2 = CF_3$; n = 5) calculated by DFT UB3LYP*/6-311++G(d,p) method.
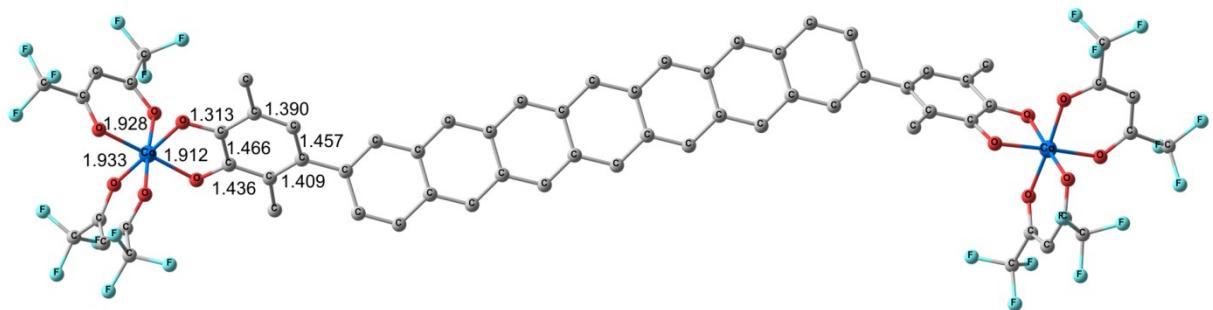
25 $_{LS}Co^{III}SQ$-$[C]_n$-$SQ_{LS}Co^{III}$
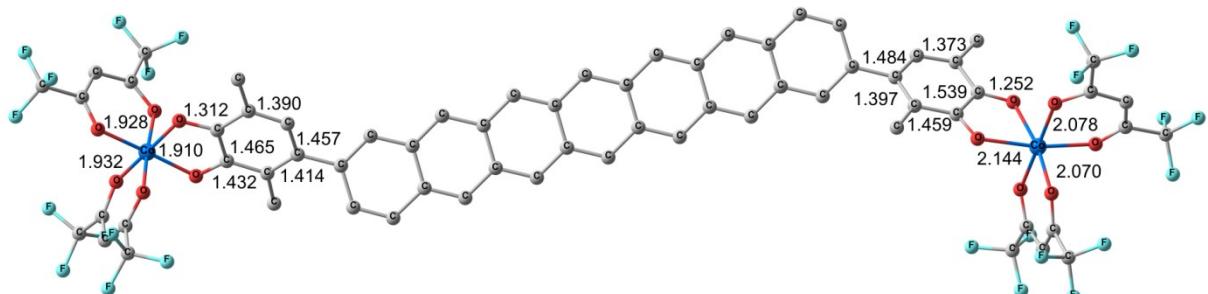
26 $_{LS}Co^{III}SQ$-$[C]_n$-$Q_{HS}Co^{II}$
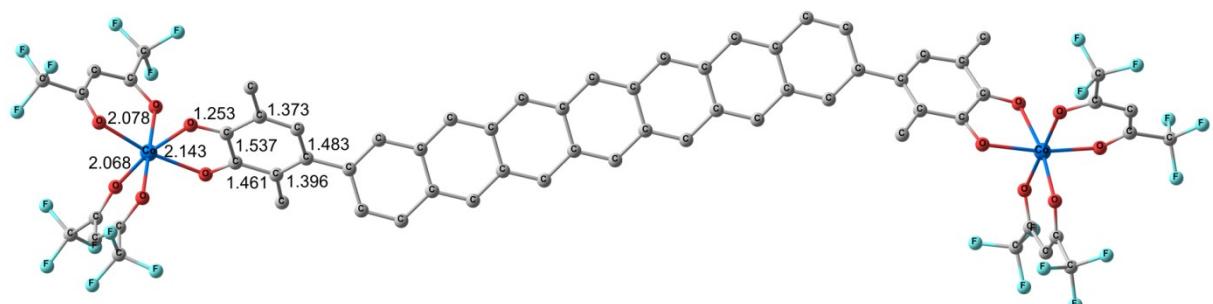

27 $_{HS}Co^{II}Q$-$[C]_n$-$Q_{HS}Co^{II}$

Figure S10. Optimized geometries of the electromers of the adduct **I** ($R_1 = R_2 = CF_3$; $n = 5$) calculated by DFT UB3LYP*/6-311++G(d,p) method.

o-Quinone derivatives of the acenes Q2 and complexes II

Table S5. Multiplicities (*Ms*), total energies (*E*), relative energies (Δ*E*), expectation values of the spin-squared operator (S^2) and spin coupling constants (J ([C]$_n$-[C]$_n$)) in the compounds **Q2** (n=5–7) calculated by DFT UB3LYP/6-311++G(d,p) method.

Structure	*Ms*	E_{total}, a. u.	Δ*E*, kcal mol^{-1}	S^2	J ([C]$_n$-[C]$_n$), cm^{-1}
Q2 (n=5)	3	-1452.83547		2.046	-1180
BS	1	-1452.84005	2.9	1.193	
Q2 (n=6)	3	-1606.50516		2.049	-1734
BS	1	-1606.51138	3.9	1.262	
Q2 (n=7)	3	-1760.17381		2.071	-2596
BS	1	-1760.18191	5.1	1.387	

n=5

n=6

n=7
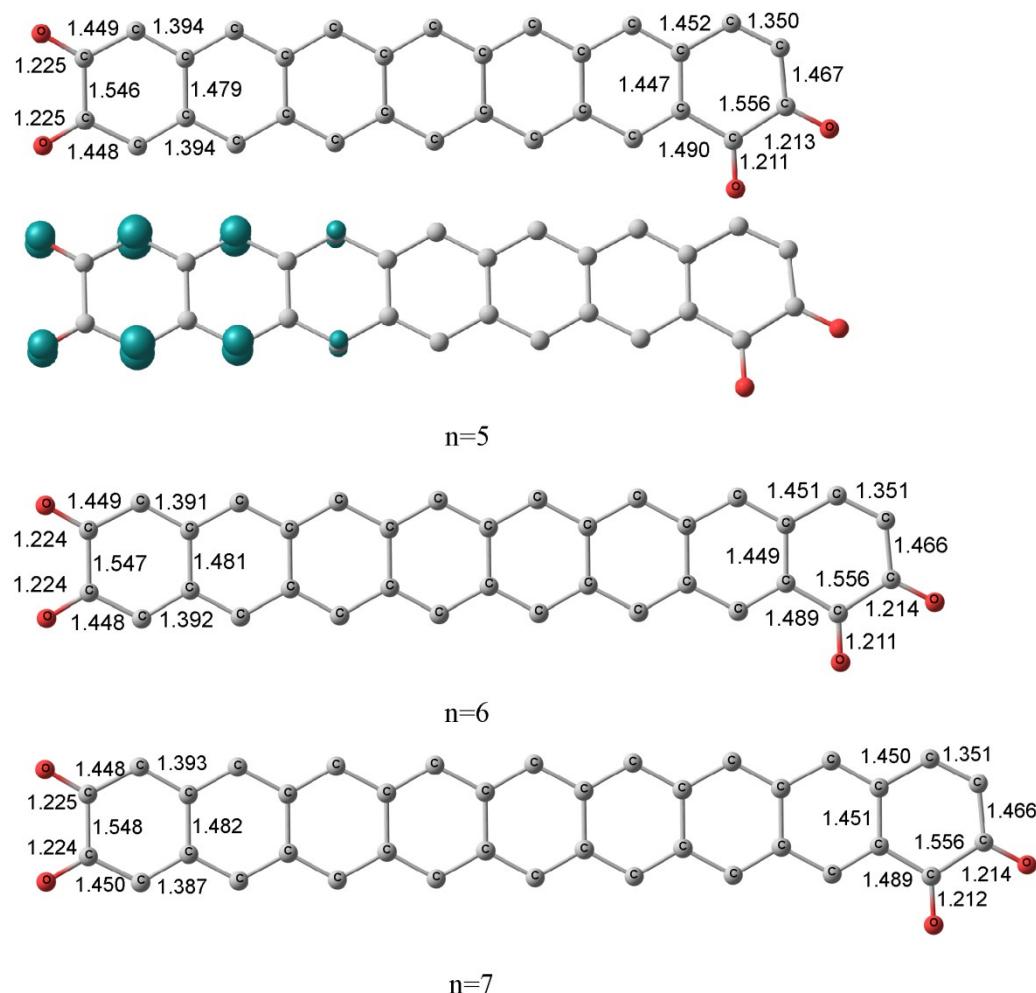
Figure S11. Optimized geometries of the compounds **Q2** (n=5–7) and spin density distribution in the **Q2** (n=5) calculated by DFT UB3LYP/6-311++G(d,p) method.

Table S6. Multiplicities (Ms), total energies (E_{total}), stabilization energies (E_{stab}), relative energies (ΔE), expectation values of the spin-squared operator (S^2), exchange spin coupling constants (J) in the electromers of the adducts **II** (R_1, R_2 = CH_3, CF_3; n = 1) calculated by the DFT B3LYP*/6-311++$G(d, p)$ method.

| Structure	Ms	E_{total}, a. u.	E_{stab}, kcal mol^{-1}	ΔE, kcal mol^{-1}	S^2	J, cm^{-1}
R$_1$=R$_2$=CH$_3$						
28 $_{LS}$Co^{III}SQ-[C]$_n$-[C]$_n$-SQ$_{LS}$Co^{III}	1	-4965.08841	47.4	0.0	0.000	
29 $_{LS}$Co^{III}SQ-[C]$_n$-[C]$_n$-Q$_{HS}$Co^{II}	5	-4965.06526	32.9	14.5	6.019	
29 BS	3	-4965.06539	33.0	14.4	3.089	-10
30 $_{HS}$Co^{III}SQ-[C]$_n$-[C]$_n$-SQ$_{LS}$Co^{III}	5	-4965.06309	31.6	15.9	6.037	
31 $_{HS}$Co^{III}SQ-[C]$_n$-[C]$_n$-Q$_{HS}$Co^{II}	9	-4965.03656	14.9	32.5	20.122	
R$_1$=CH$_3$, R$_2$=CF$_3$						
32 $_{LS}$Co^{III}SQ-[C]$_n$-[C]$_n$-SQ$_{LS}$Co^{III}	1	-6150.52686	47.4	0.0	0.000	
33 $_{LS}$Co^{III}SQ-[C]$_n$-[C]$_n$-Q$_{HS}$Co^{II}	5	-6150.51090	37.4	10.0	6.065	
33 BS	3	-6150.51102	37.5	9.9	3.088	-9
34 $_{HS}$Co^{III}SQ-[C]$_n$-[C]$_n$-SQ$_{LS}$Co^{III}	5	-6150.50484	33.6	13.8	6.050	
35 $_{HS}$Co^{III}SQ-[C]$_n$-[C]$_n$-Q$_{HS}$Co^{II}	9	-6150.48579	21.6	25.8	20.232	
R$_1$=R$_2$=CF$_3$						
36 $_{LS}$Co^{III}SQ-[C]$_n$-[C]$_n$-SQ$_{LS}$Co^{III}	1	-7335.94518	48.3	0.0	0.000	
37 $_{LS}$Co^{III}SQ-[C]$_n$-[C]$_n$-Q$_{HS}$Co^{II}	5	-7335.93658	42.9	5.4	6.042	
37 BS	3	-7335.93670	43.0	5.3	3.051	-9
38 $_{HS}$Co^{III}SQ-[C]$_n$-[C]$_n$-SQ$_{LS}$Co^{III}	5	-7335.92749	37.2	11.1	6.060	
39 $_{HS}$Co^{III}SQ-[C]$_n$-[C]$_n$-Q$_{HS}$Co^{II}	9	-7335.90909	25.6	22.6	20.095	

28 LSCoIIISQ-[C]n-[C]n-SQLSCoIII

29 LSCoIIISQ-[C]n-[C]n-QHSCoII

30 HSCoIIISQ-[C]n-[C]n-SQLSCoIII

31 HSCoIIISQ-[C]n-[C]n-QHSCoII
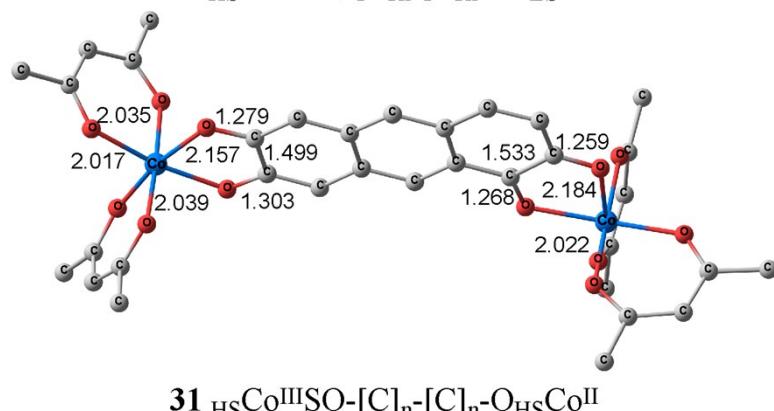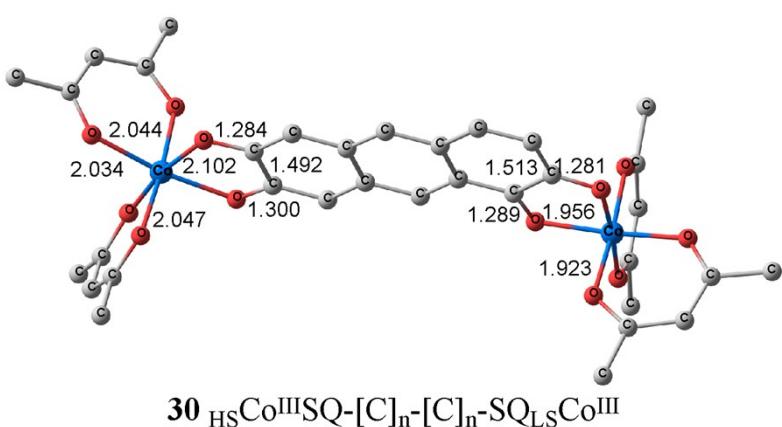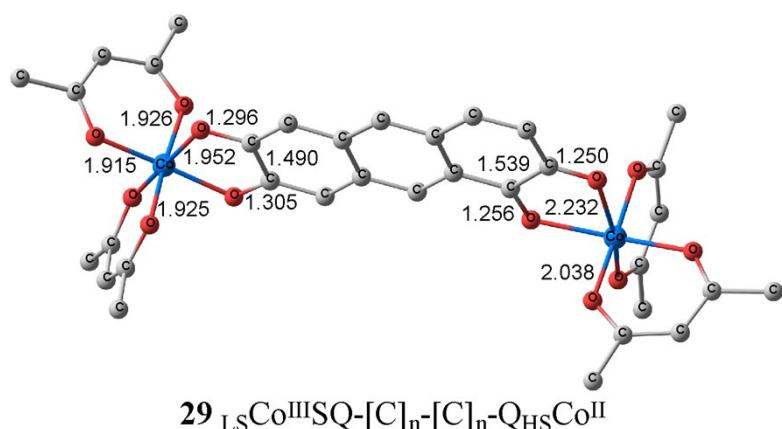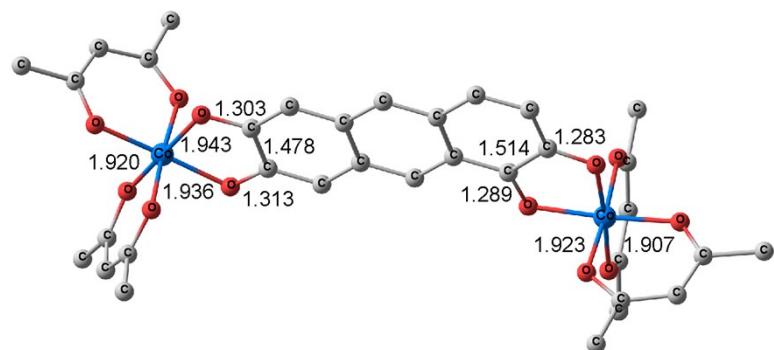
Figure S12. Optimized geometries of the electromers of the adduct **II** ($R_1 = R_2 = CH_3$; n = 1) calculated by DFT UB3LYP*/6-311++G(d,p) method.

**32** $_{LS}Co^{III}SQ$-$[C]_n$-$[C]_n$-$SQ_{LS}Co^{III}$

**33** $_{LS}Co^{III}SQ$-$[C]_n$-$[C]_n$-$Q_{HS}Co^{II}$

**34** $_{HS}Co^{III}SQ$-$[C]_n$-$[C]_n$-$SQ_{LS}Co^{III}$


35 $_{HS}Co^{III}SQ$-$[C]_n$-$[C]_n$-$Q_{HS}Co^{II}$
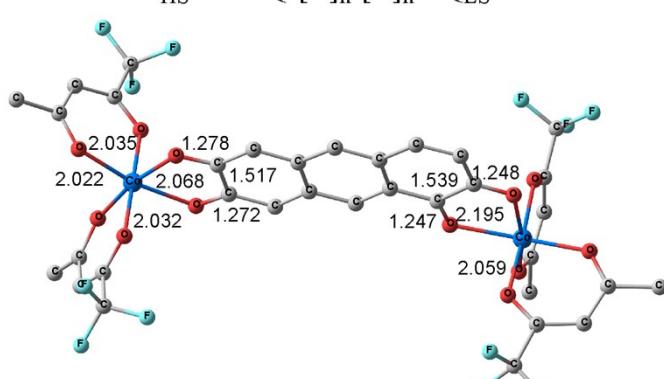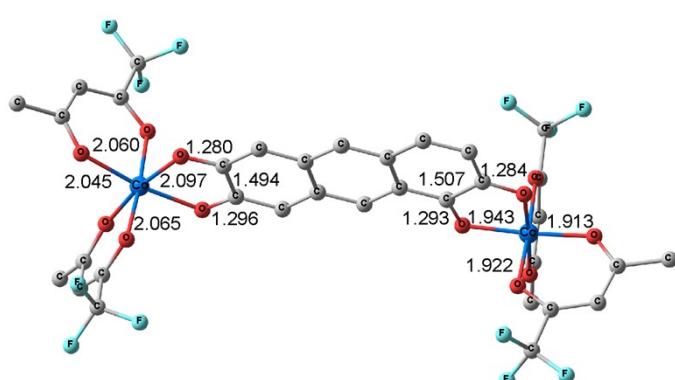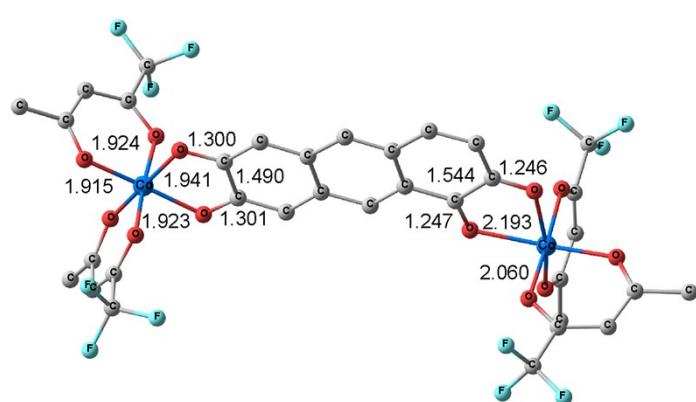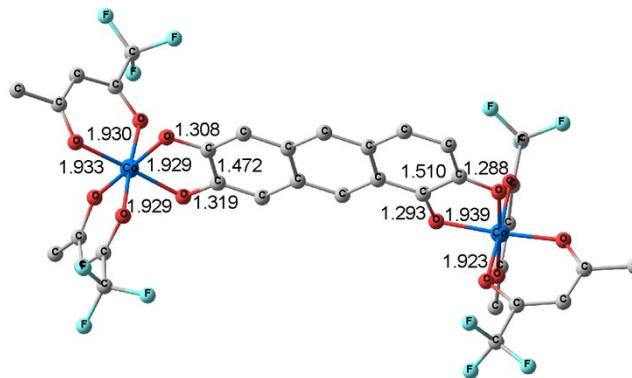
Figure S13. Optimized geometries of the electromers of the adduct **II** ($R_1 = CH_3$, $R_2 = CF_3$; n =1) calculated by DFT UB3LYP*/6-311++G(d,p) method.
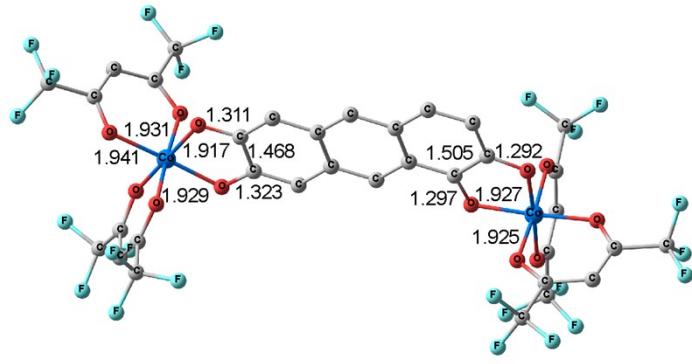
36 $_{LS}Co^{III}SQ$-$[C]_n$-$[C]_n$-$SQ_{LS}Co^{III}$
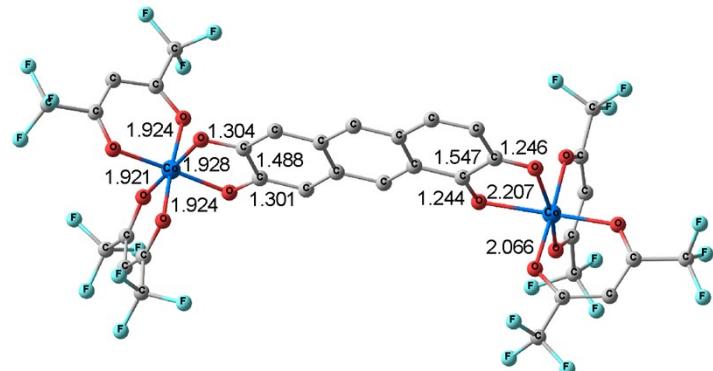
37 $_{LS}Co^{III}SQ$-$[C]_n$-$[C]_n$-$Q_{HS}Co^{II}$
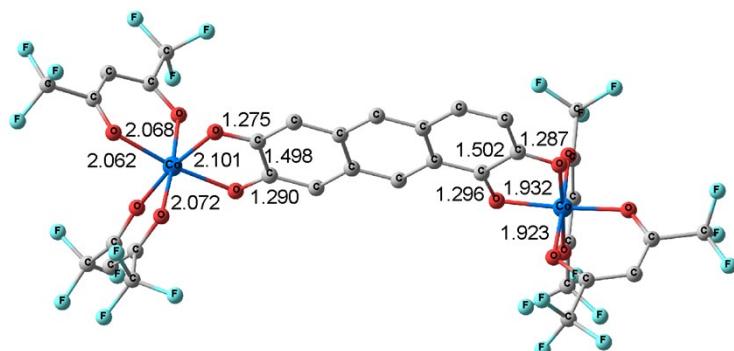
38 $_{HS}Co^{III}SQ$-$[C]_n$-$[C]_n$-$SQ_{LS}Co^{III}$
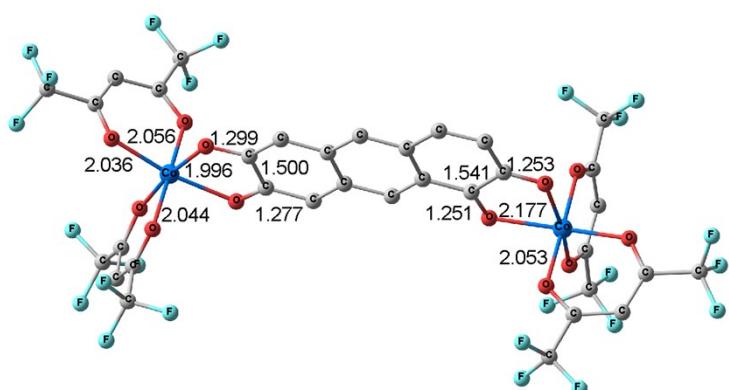
39 $_{HS}Co^{III}SQ$-$[C]_n$-$[C]_n$-$Q_{HS}Co^{II}$

Figure S14. Optimized geometries of the electromers of the adduct **II** ($R_1 = R_2 = CF_3$; $n = 1$) calculated by DFT UB3LYP*/6-311++G(d,p) method.

**Table S7**. Multiplicities (Ms), total energies (E_{total}), stabilization energies (E_{stab}), relative energies (ΔE), expectation values of the spin-squared operator (S^2), exchange spin coupling constants (J) in the electromers of the adducts **II** (R$_1$, R$_2$ = CH$_3$, CF$_3$; n = 3) calculated by the DFT B3LYP*/6-311++$G(d, p)$ method.

Structure	Ms	E_{total}, a. u.	E_{stab}, kcal mol^{-1}	ΔE, kcal mol^{-1}	S^2	J, cm^{-1}
R$_1$=R$_2$=CH$_3$						
40 $_{LS}$Co^{III}SQ-[C]$_n$-[C]$_n$-SQ$_{LS}$Co^{III}	1	-5270.29129	61.9	0.0	0.000	
41 $_{LS}$Co^{III}SQ-[C]$_n$-[C]$_n$-Q$_{HS}$Co^{II}	5	-5270.27094	49.2	12.8	6.207	
41 BS	3	-5270.26708	46.7	15.2	3.208	286
42 $_{HS}$Co^{III}SQ-[C]$_n$-[C]$_n$-SQ$_{LS}$Co^{III}	7	-5270.25691	40.4	21.6	12.044	
43 $_{HS}$Co^{III}SQ-[C]$_n$-[C]$_n$-Q$_{HS}$Co^{II}	9	-5270.24461	32.6	29.3	20.246	
R$_1$=CH$_3$, R$_2$=CF$_3$						
44 $_{LS}$Co^{III}SQ-[C]$_n$-[C]$_n$-SQ$_{LS}$Co^{III}	1	-6455.73133	62.9	0.0	0.000	
45 $_{LS}$Co^{III}SQ-[C]$_n$-[C]$_n$-Q$_{HS}$Co^{II}	5	-6455.71914	55.2	7.7	6.108	
45 BS	3	-6455.71761	54.3	8.6	3.079	111
46 $_{HS}$Co^{III}SQ-[C]$_n$-[C]$_n$-SQ$_{LS}$Co^{III}	7	-6455.70065	43.6	19.3	12.044	
47 $_{HS}$Co^{III}SQ-[C]$_n$-[C]$_n$-Q$_{HS}$Co^{II}	9	-6455.69584	40.6	22.3	20.145	
R$_1$=R$_2$=CF$_3$						
48 $_{LS}$Co^{III}SQ-[C]$_n$-[C]$_n$-SQ$_{LS}$Co^{III}	1	-7641.15218	65.4	0.0	0.000	
49 $_{LS}$Co^{III}SQ-[C]$_n$-[C]$_n$-Q$_{HS}$Co^{II}	5	-7641.14818	62.8	2.5	6.067	
49 BS	3	-7641.14727	62.3	3.1	3.051	66
50 $_{HS}$Co^{III}SQ-[C]$_n$-[C]$_n$-SQ$_{LS}$Co^{III}	7	-7641.12617	49.0	16.3	12.043	
51 $_{HS}$Co^{III}SQ-[C]$_n$-[C]$_n$-Q$_{HS}$Co^{II}	9	-7641.12925	51.0	14.4	20.056	

40 $_{LS}Co^{III}SQ-[C]_n-[C]_n-SQ_{LS}Co^{III}$

41 $_{LS}Co^{III}SQ-[C]_n-[C]_n-Q_{HS}Co^{II}$

42 $_{HS}Co^{III}SQ-[C]_n-[C]_n-SQ_{LS}Co^{III}$


43 $_{HS}Co^{III}SQ-[C]_n-[C]_n-Q_{HS}Co^{II}$
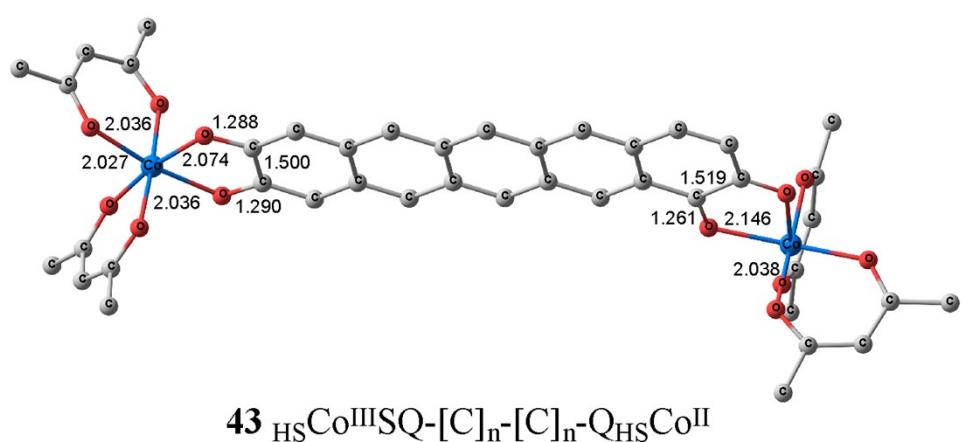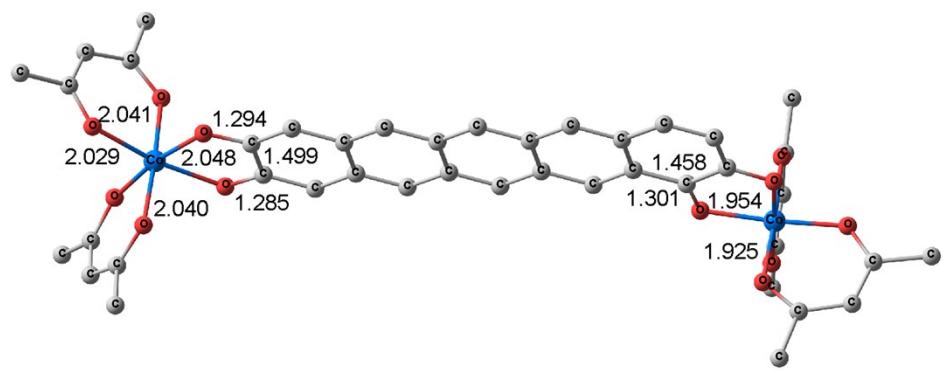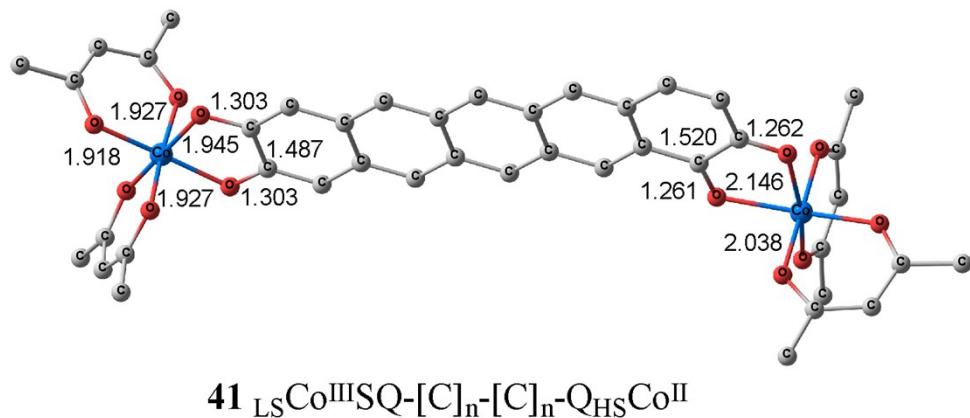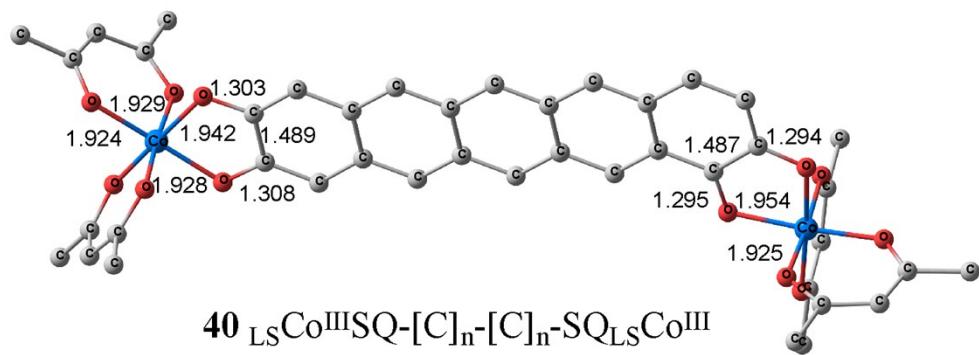
Figure S15. Optimized geometries of the electromers of the adduct **II** ($R_1 = R_2 = CH_3$; $n = 3$) calculated by DFT UB3LYP*/6-311++G(d,p) method.

44 $_{LS}Co^{III}SQ-[C]_n-[C]_n-SQ_{LS}Co^{III}$

45 $_{LS}Co^{III}SQ-[C]_n-[C]_n-Q_{HS}Co^{II}$

46 $_{HS}Co^{III}SQ-[C]_n-[C]_n-SQ_{LS}Co^{III}$

47 $_{HS}Co^{III}SQ-[C]_n-[C]_n-Q_{HS}Co^{II}$
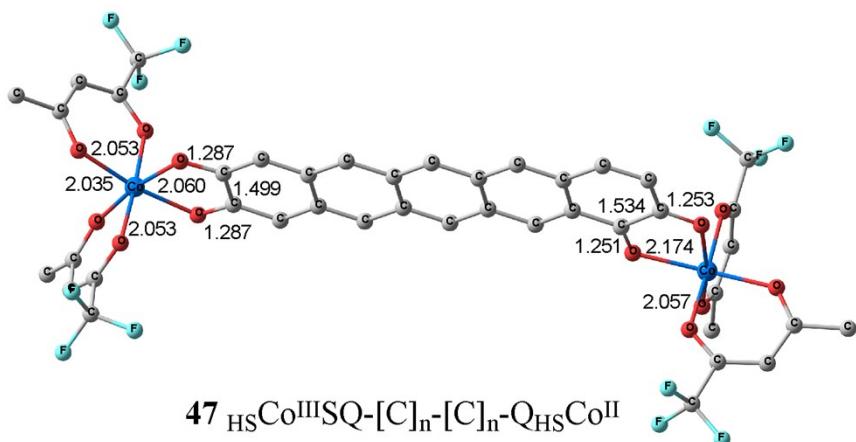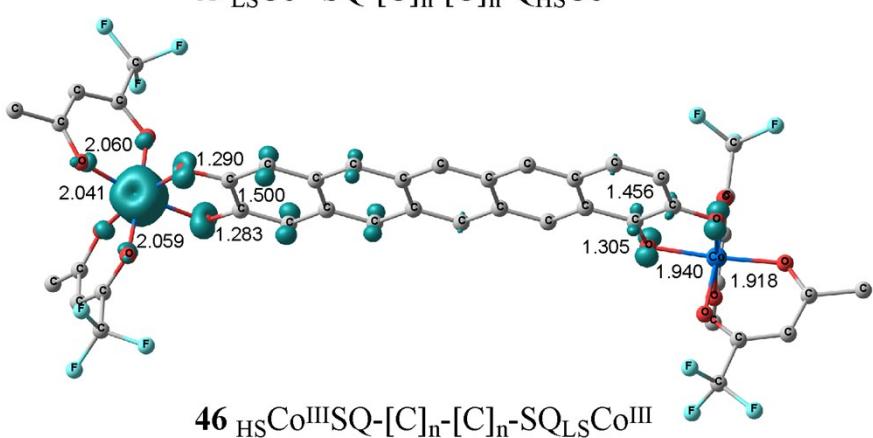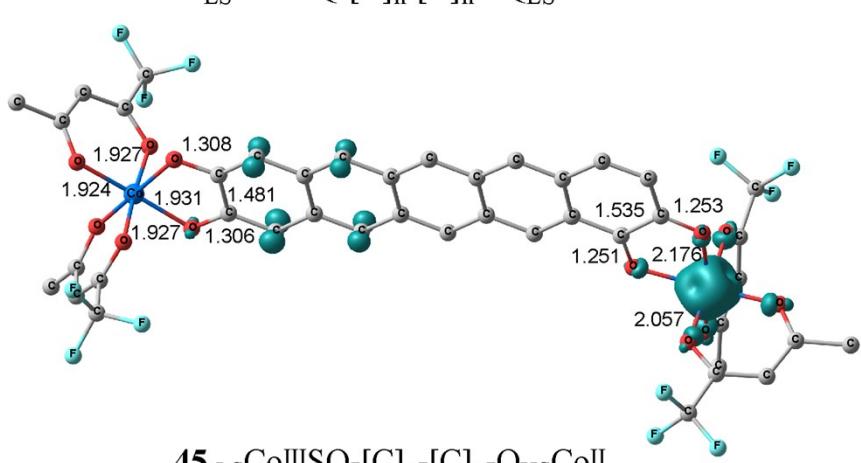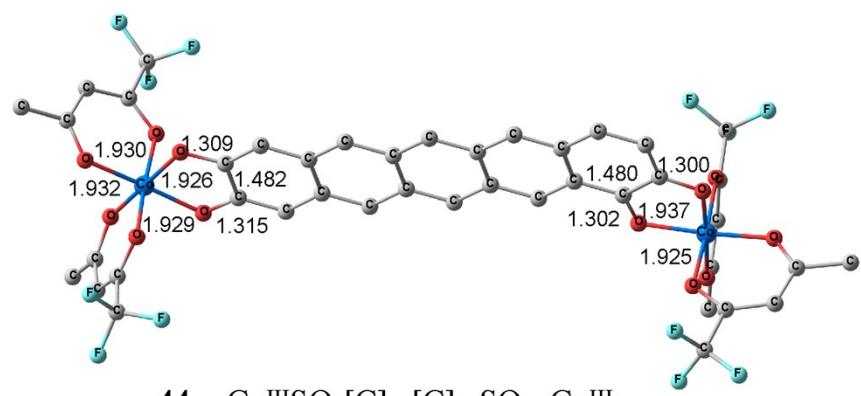
Figure S16. Optimized geometries and spin density distribution in the electromers of the adduct **II** ($R_1 = CH_3$, $R_2 = CF_3$; n=3) calculated by DFT UB3LYP*/6-311++G(d,p) method.

48 LSCoIIISQ-[C]n-[C]n-SQLSCoIII

49 LSCoIIISQ-[C]n-[C]n-QHSCoII

50 HSCoIIISQ-[C]n-[C]n-SQLSCoIII

51 HSCoIIISQ-[C]n-[C]n-QHSCoII
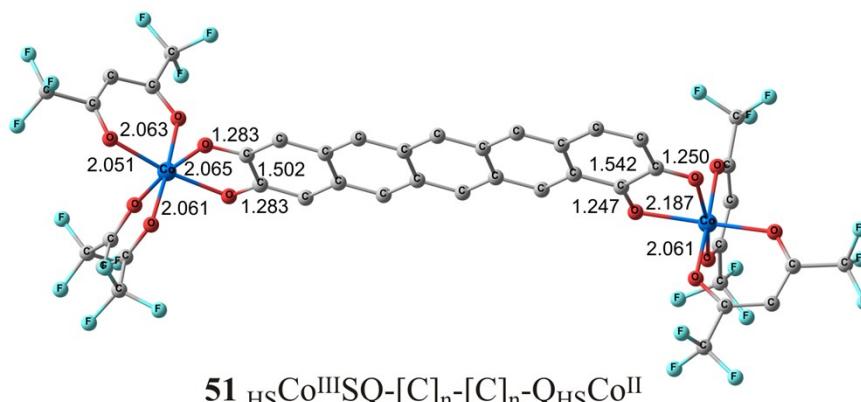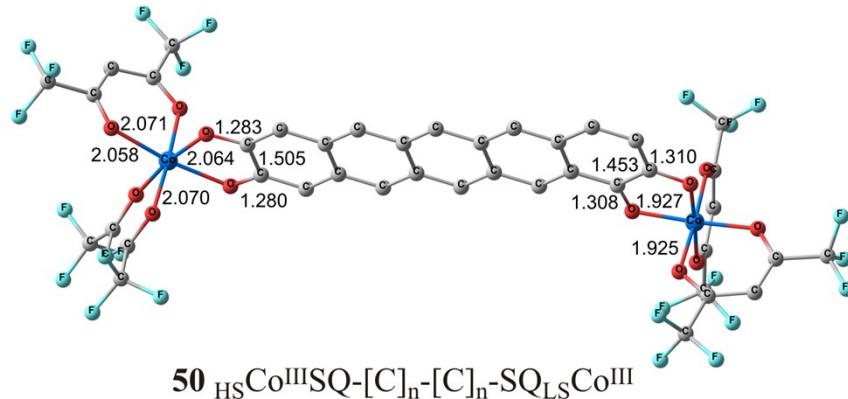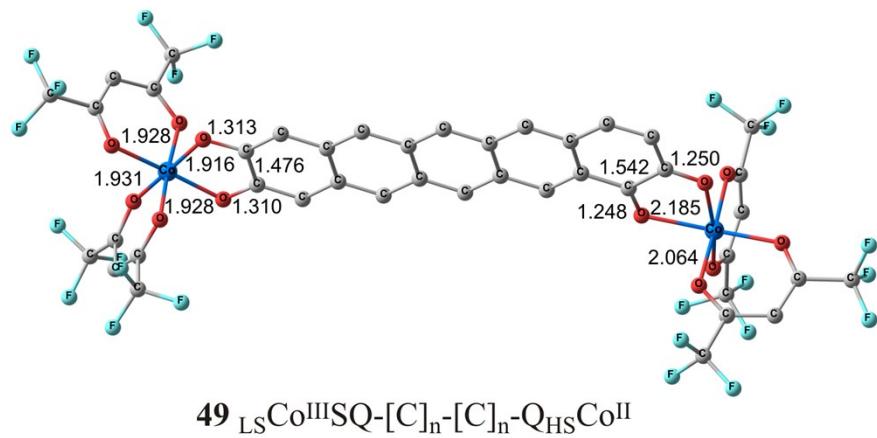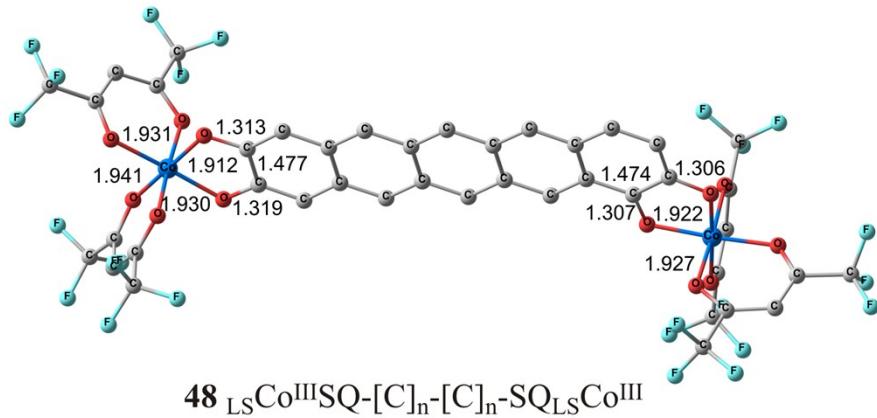
Figure S17. Optimized geometries of the electromers of the adduct **II** ($R_1 = R_2 = CF_3$; n = 3) calculated by DFT UB3LYP*/6-311++G(d,p) method.

Table S8. Multiplicities (Ms), total energies (E_{total}), stabilization energies (E_{stab}), relative energies (ΔE), expectation values of the spin-squared operator (S^2), exchange spin coupling constants (J) in the electromers of the adducts **II** (R_1, R_2 = CH$_3$, CF$_3$; n = 5) calculated by the DFT B3LYP*/6-311++$G(d, p)$ method.

| Structure	Ms	E_{total}, a. u.	E_{stab}, kcal mol^{-1}	ΔE, kcal mol^{-1}	S^2	J, cm^{-1}
R$_1$=R$_2$=CH$_3$						
52a $_{LS}$Co^{III}SQ-[C]$_n$-[C]$_n$-SQ$_{LS}$Co^{III}	5	-5575.45003	21.1	24.5	6.035	
52b $_{LS}$Co^{III}SQ-[C]$_n$-[C]$_n$-SQ$_{LS}$Co^{III}	3	-5575.48543	43.3	2.3	2.040	
52 BS	1	-5575.48908	45.6	0.0	0.783	-636
53a $_{LS}$Co^{III}SQ-[C]$_n$-[C]$_n$-Q$_{HS}$Co^{II}	7	-5575.45403	23.6	22.0	12.051	
53b $_{LS}$Co^{III}SQ-[C]$_n$-[C]$_n$-Q$_{HS}$Co^{II}	5	-5575.47247	35.2	10.4	6.215	
53 BS	3	-5575.47132	34.4	11.1	3.208	84
54 $_{HS}$Co^{III}SQ-[C]$_n$-[C]$_n$-SQ$_{LS}$Co^{III}	7	-5575.46279	29.1	16.5	12.028	
55 $_{HS}$Co^{III}SQ-[C]$_n$-[C]$_n$-Q$_{HS}$Co^{II}	9	-5575.44615	18.6	26.9	20.250	–
R$_1$=CH$_3$, R$_2$=CF$_3$						
56a $_{LS}$Co^{III}SQ-[C]$_n$-[C]$_n$-SQ$_{LS}$Co^{III}	5	-6760.88878	21.2	26.1	6.035	
56b $_{LS}$Co^{III}SQ-[C]$_n$-[C]$_n$-SQ$_{LS}$Co^{III}	3	-6760.92664	45.0	2.4	2.040	
56 BS	1	-6760.93045	47.4	0.0	0.770	-660
57a $_{LS}$Co^{III}SQ-[C]$_n$-[C]$_n$-Q$_{HS}$Co^{II}	7	-6760.88724	20.3	27.1	12.083	
57b $_{LS}$Co^{III}SQ-[C]$_n$-[C]$_n$-Q$_{HS}$Co^{II}	5	-6760.92363	43.1	4.3	6.093	
57 BS	3	-6760.92301	42.8	4.6	3.080	42
58 $_{HS}$Co^{III}SQ-[C]$_n$-[C]$_n$-SQ$_{LS}$Co^{III}	7	-6760.90420	30.9	16.5	12.056	
59 $_{HS}$Co^{III}SQ-[C]$_n$-[C]$_n$-Q$_{HS}$Co^{II}	9	-6760.89842	27.3	20.1	20.136	–
R$_1$=R$_2$=CF$_3$						
60a $_{LS}$Co^{III}SQ-[C]$_n$-[C]$_n$-SQ$_{LS}$Co^{III}	5	-7946.31462	26.8	25.2	6.035	
60b $_{LS}$Co^{III}SQ-[C]$_n$-[C]$_n$-SQ$_{LS}$Co^{III}	3	-7946.34820	47.9	4.1	2.040	
60 BS	1	-7946.35480	52.0	0.0	0.743	-1117
61a $_{LS}$Co^{III}SQ-[C]$_n$-[C]$_n$-Q$_{HS}$Co^{II}	7	-7946.31617	27.8	24.2	12.058	
61b $_{LS}$Co^{III}SQ-[C]$_n$-[C]$_n$-Q$_{HS}$Co^{II}	5	-7946.35532	52.4	-0.3	6.062	
61 BS	3	-7946.35480	52.0	0.0	3.055	38
62 $_{HS}$Co^{III}SQ-[C]$_n$-[C]$_n$-SQ$_{LS}$Co^{III}	7	-7946.33170	37.5	14.5	12.054	
63 $_{HS}$Co^{III}SQ-[C]$_n$-[C]$_n$-Q$_{HS}$Co^{II}	9	-7946.33681	40.7	11.3	20.140	–
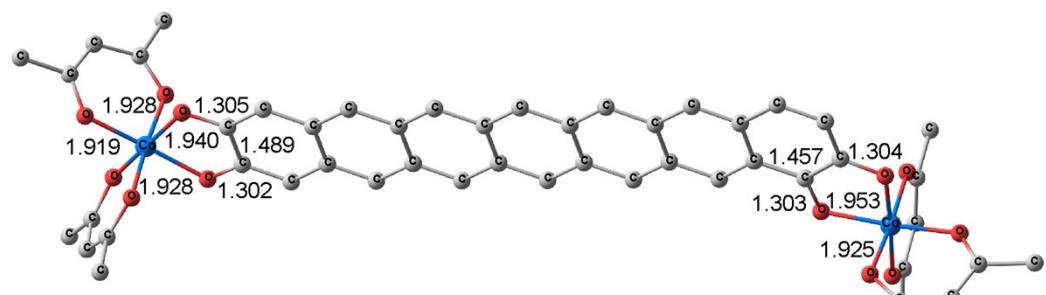
52b LSCoIIISQ-[C]n-[C]n-SQLSCoIII
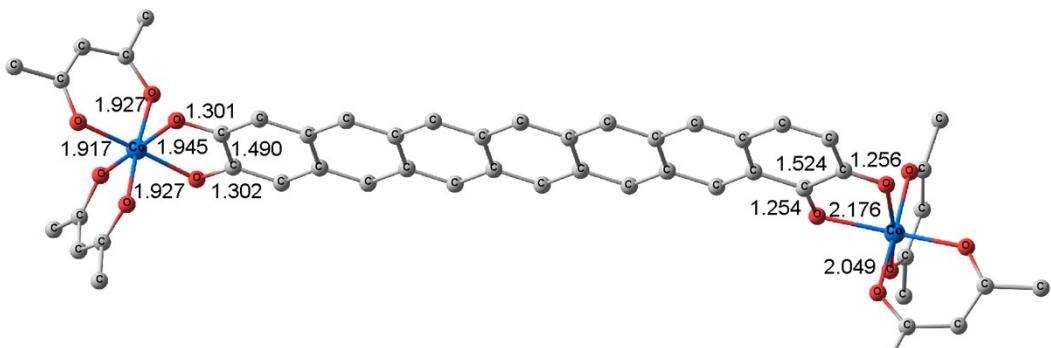
53b LSCoIIISQ-[C]n-[C]n-QHSCoII
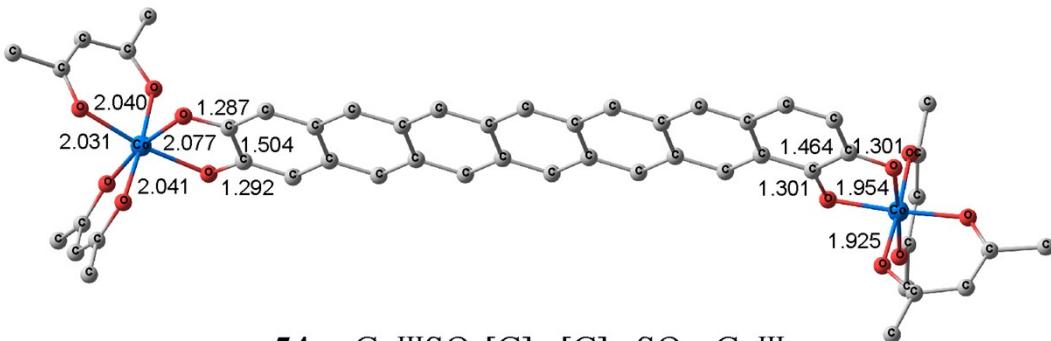
54 HSCoIIISQ-[C]n-[C]n-SQLSCoIII
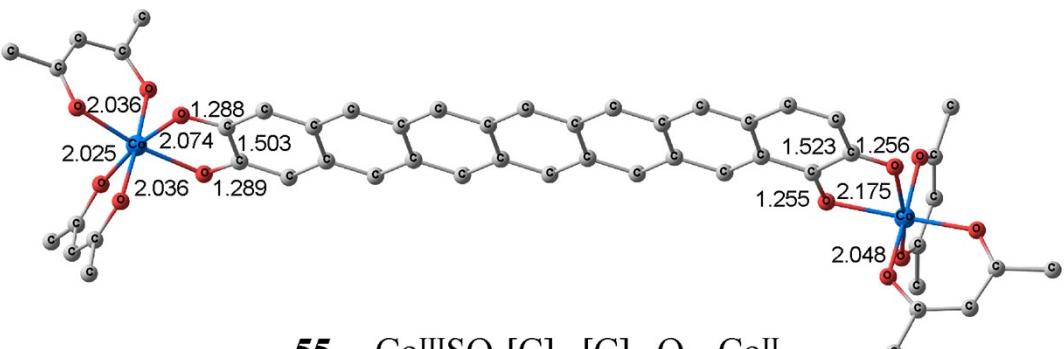
55 HSCoIIISQ-[C]n-[C]n-QHSCoII

Figure S18. Optimized geometries of the electromers of the adduct **II** ($R_1 = R_2 = CH_3$; n = 5) calculated by DFT UB3LYP*/6-311++G(d,p) method.
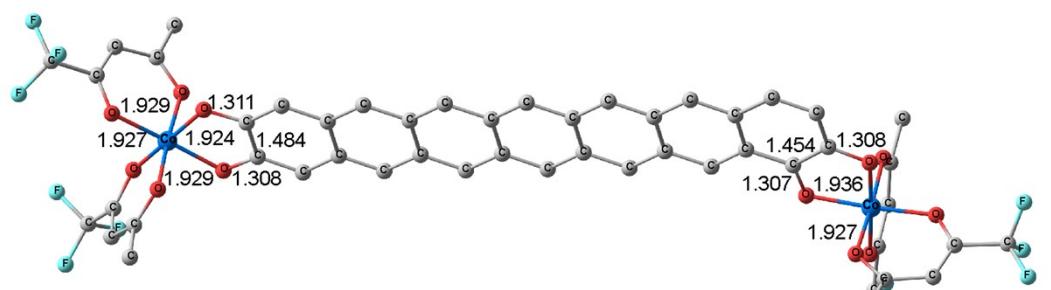
56b $_{LS}Co^{III}SQ$-$[C]_n$-$[C]_n$-$SQ_{LS}Co^{III}$
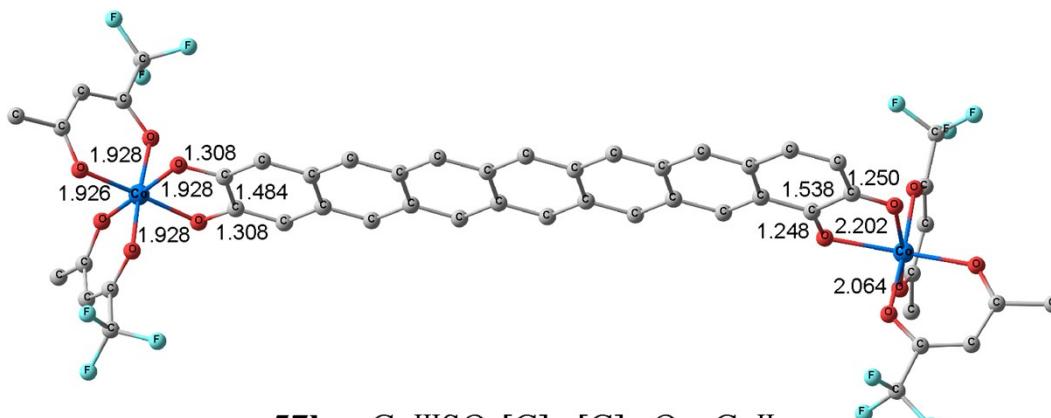
57b $_{LS}Co^{III}SQ$-$[C]_n$-$[C]_n$-$Q_{HS}Co^{II}$
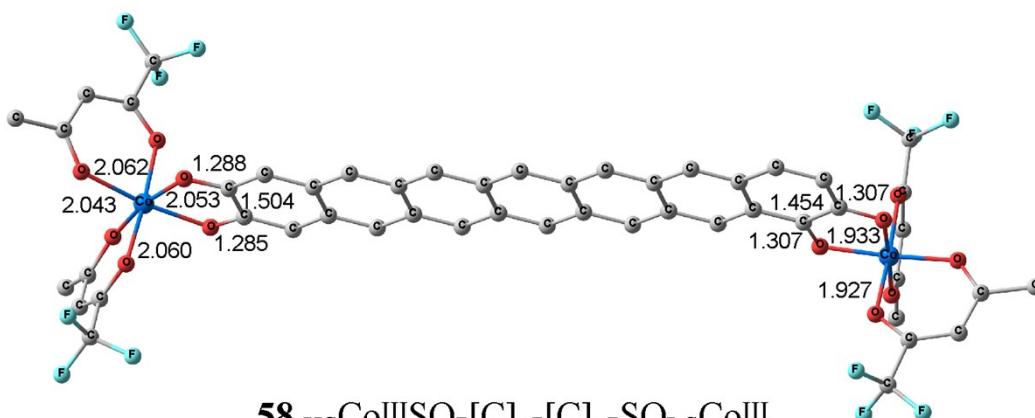
58 $_{HS}Co^{III}SQ$-$[C]_n$-$[C]_n$-$SQ_{LS}Co^{III}$
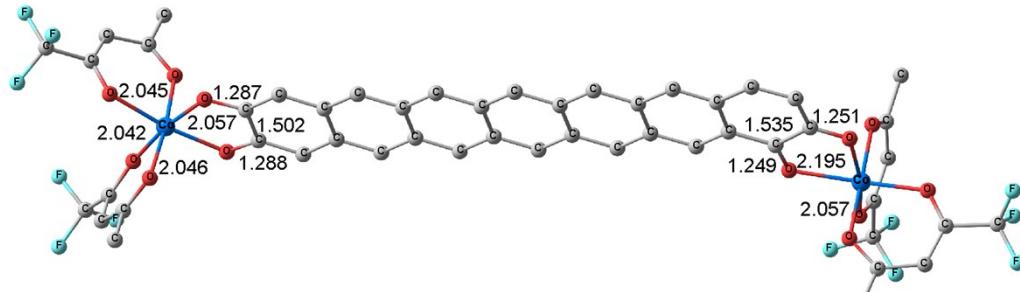
59 $_{HS}Co^{III}SQ$-$[C]_n$-$[C]_n$-$Q_{HS}Co^{II}$

Figure S19. Optimized geometries of the electromers of the adduct **II** ($R_1 = CH_3$, $R_2 = CF_3$; n=5) calculated by DFT UB3LYP*/6-311++G(d,p) method.
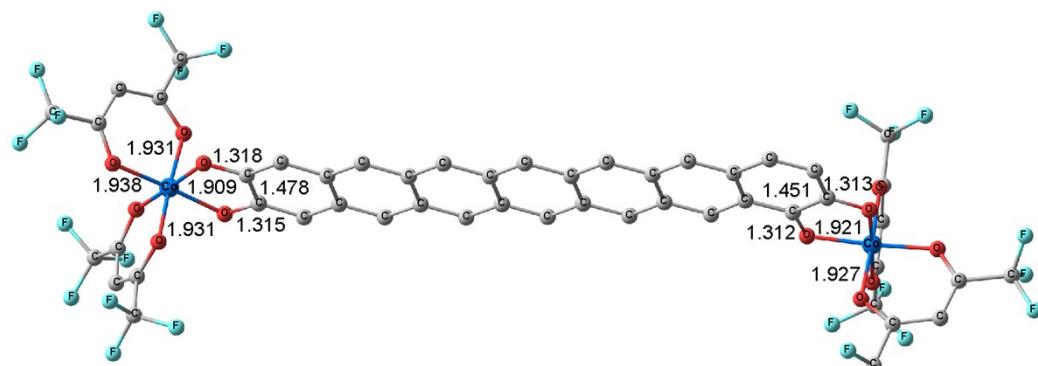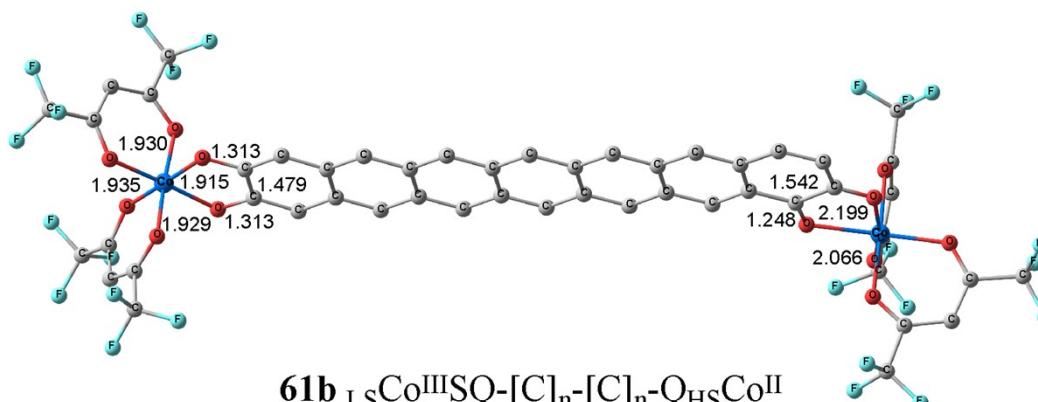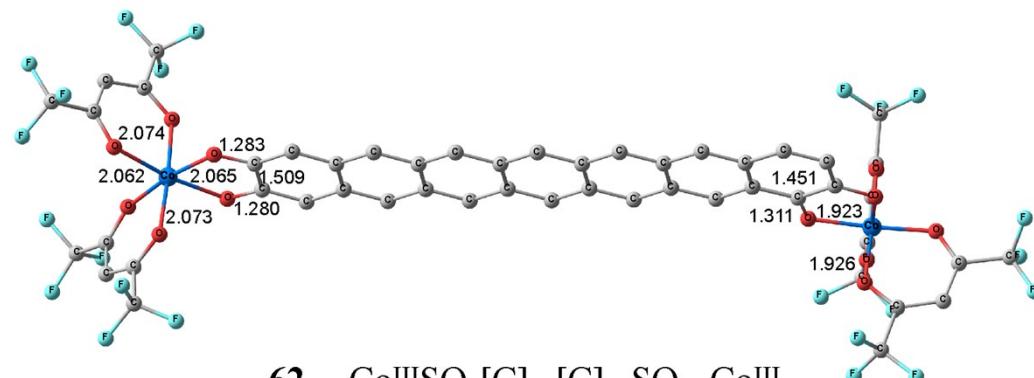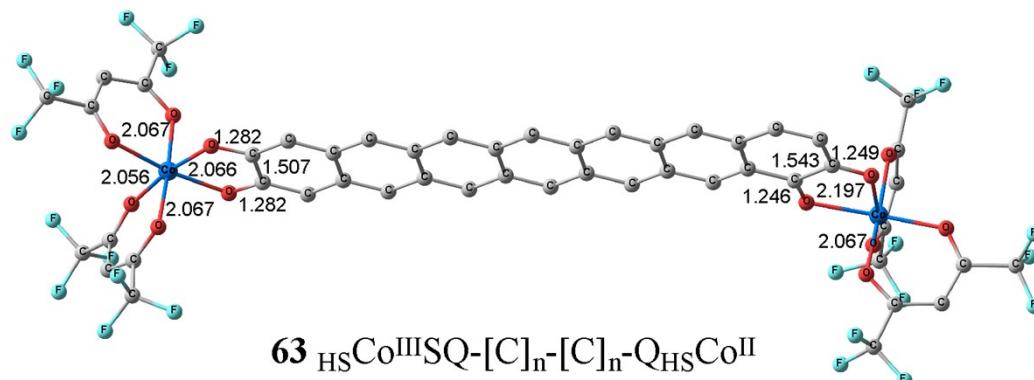
Figure S20. Optimized geometries of the electromers of the adduct **II** ($R_1 = R_2 = CF_3$; $n = 5$) calculated by DFT UB3LYP*/6-311++G(d,p) method.

Table S9. Rotation angle of the quinone rings relative to the acene linker, total energy in the high-spin state (E_{HS}), total energy in the broken symmetry state (E_{BS}), expectation value of the spin-squared operator in the high-spin state (S^2_{HS}), expectation value of the spin-squared operator in the broken symmetry state (S^2_{BS}) and exchange spin coupling constant (J) in the $_{LS}Co^{III}$SQ-[C]$_n$-[C]$_n$-SQ$_{LS}Co^{III}$ electromer of the adduct **I** (R_1, R_2 = CH_3; n = 1) calculated by the DFT B3LYP*/6-311++$G(d, p)$ method.

Rotation angle*,°	E_{HS}, a.u.	E_{BS}, a.u.	S^2_{HS}	S^2_{BS}	J, cm^{-1}
-10	-5604.664242	-5604.664437	2.0170	1.0169	−42.8
0 (opt)	-5580.179142	-5580.179245	2.0117	1.0094	−22.5
10	-5604.664564	-5604.664598	2.0167	1.0168	−7.4
20	-5604.662843	-5604.662849	2.0166	1.0166	−1.4
30	-5604.661427	-5604.661427	2.0166	1.0166	0.0

* Rotation angle is given relative to the optimized value of the angle (52°)